THE 3D-INDEX OF THE 3D-SKEIN MODULE VIA THE QUANTUM TRACE MAP

STAVROS GAROUFALIDIS AND TAO YU

ABSTRACT. We define a map from the skein module of a cusped hyperbolic 3-manifold to the ring of Laurent series in one variable with integer coefficients that satisfies two properties: its evaluation at peripheral curves coincides with the Dimofte–Gaiotto–Gukov 3d-index, and it factors through the 3d-quantum trace map associated to a suitable ideal triangulation of the manifold. The map fulfills a supersymmetry prediction of mathematical physics and is part of a conjectural 3+1 dimensional topological quantum field theory.

CONTENTS

1. Introduction

1.1. Skein modules, quantum trace map and the 3d-index.

The paper concerns the extension of an interesting power series invariant of knots, the 3d-index of Dimofte–Gaiotto–Gukov [DGG13] to the skein module of the knot complement, using crucially a recently developed 3d-quantum trace map [GY, PP].

Recall that the skein module $\mathcal{S}(M)$ of an oriented, connected 3-manifold M, introduced in the early days of quantum topology by Przytycki [Prz91] and Turaev [Tur88], is a geometrically defined version of the $\mathrm{PSL}_2(\mathbb{C})$-character variety of $\pi_1(M)$. Its spanning set is the set of unoriented links in M and the local relations are on the one hand motivated by the recursion relations for the Jones polynomial of a knot in S^3, and on the other hand are deformations of the trace identity for 2×2 matrices.

The skein module of a 3-manifold plays an important role in topological quantum field theories (in short, TQFTs) in both $2+1$ and $3+1$ dimensions. Indeed, it is well-known that the Reshetikhin–Turaev invariant of links in an integer homology 3-sphere M is part of a 2+1 dimensional TQFT and defines a map

$$Z_{M,\omega} : \mathcal{S}(M) \to \mathbb{Z}[\omega] \tag{1}$$

for a root of unity ω [RT91, Tur94]. A repackaging of the collection of the above maps indexed by complex roots of unity to a single element of the Habiro ring is possible using Habiro's work [Hab08]; see also [GL].

The next concept is the 3d-index of Dimofte–Gaiotto–Gukov which roughly speaking sign-counts states in a supersymmetric field theory using ideas from a 3d-3d correspondence of mathematical physics, and organizes the count in a Laurent series in $\mathbb{Z}((q^{1/2}))$ with integer coefficients [DGG13, DGG14]. This series is presented as a lattice sum of products of building blocks (the tetrahedron index), and depends on a suitable ideal triangulation of a 3-manifold M with torus boundary, as well as on a choice of an integral homology basis of boundary curves. As was predicted by physics, this DGG 3d-index was shown to be a topological invariant of cusped hyperbolic 3-manifolds [GHRS15].

The 3d-3d correspondence and its $\mathcal{N} = 2$-supersymmetry algebra predicts not only the existence of the 3d-index associated to an ideal triangulation $\mathcal{T}$, but also to a module $\widehat{\mathcal{G}}(\mathcal{T})$ of operators which are roughly speaking, a left/right quotient of a ring of polynomials in q-commuting variables (i.e., of a quantum torus). This was discussed in several contexts in the physics literature; see for example [Dim16] and [AGLR]. A mathematical definition of this module that and its corresponding 3d quantum-trace map was given independently by

Panich–Park and the authors [GY, PP], both definitions using as input an ideal triangulation of the ambient 3-manifold.

But the $\mathcal{N} = 2$-supersymmetry algebra predicts more, namely an extension of the 3d-index to the skein module with two properties:

(a) when evaluated on the peripheral part of the skein module coincides with the DGG 3d-index.

(b) it factors through the quantum trace map.

This prediction is discussed in detail by Agarwal–Gang–Lee–Romo [AGLR], based on earlier work [GKRY16, Sec.5].

The goal of the paper is to mathematically fulfill this prediction. In fact, the map (2) defined below concerns a 3+1 dimensional aspect of the skein module $\mathcal{S}(M)$. Indeed, Witten conjectured the existence of a 3+1 dimensional TQFT whose vector space associated to a 3-manifold M is the skein module $\mathcal{S}(M)$. The finiteness of the rank of this module, conjectured by Witten, was proven by Gunningham–Jordan–Safronov [GJS23] for closed 3-manifolds. Arithmetic aspects of this TQFT were phrased in terms of holomorphic quantum modular forms in [GZ], and in terms of a map from the skein module of an integer homology 3-sphere to the Habiro ring [GL, Eqn(3)] mentioned above. A full definition of this 3+1 dimensional TQFT is an interesting and challenging question which, without doubt, lead to a better understanding of 4 dimensional smooth manifolds.

1.2. **Our results.** We are now ready to formulate our results.

Theorem 1.1. *For a cusped hyperbolic 3-manifold M with no non-peripheral $\mathbb{Z}/2$-homology, there exist a map*

$$I_M : \mathcal{S}^{\mathrm{ev}}(M) \to \mathbb{Z}(\!(q^{1/2})\!) \tag{2}$$

with the following properties:

(a) *its restriction at peripheral elements agrees with the 3d-index of Dimofte–Gaiotto–Gukov:*

$$I_M(\hat{m}_\lambda^{-2m} \hat{m}_\mu^{2e}) = I_M^{\mathrm{DGG}}(m, e) . \tag{3}$$

(b) *it factors through the 3d-quantum trace map for suitable triangulations.*

Here, $\mathcal{S}^{\mathrm{ev}}(M)$ is the even part of the skein module (see Section 2.5) and the condition that M has no non-peripheral $\mathbb{Z}/2$-homology (i.e., that $H_1(\partial M; \mathbb{Z}/2) \to H_1(M; \mathbb{Z}/2)$ is surjective, which for instance is satisfied for complements of links in the 3-sphere) is a technical assumption that can be relaxed; see Remark 5.6.

A key ingredient of the above map is the 3d quantum trace map. The map I_M and the precise meaning of suitable triangulations is made clear with the next theorem and the discussion following it.

Theorem 1.2. *For every 1-efficient triangulation $\mathcal{T}$ of a cusped-hyperbolic manifold with no non-peripheral $\mathbb{Z}/2$-homology, there exists a map*

$$I_{\mathcal{T}} : \widehat{\mathcal{G}}^{\mathrm{ev}}(\mathcal{T}) \to \mathbb{Z}(\!(q^{1/2})\!) \tag{4}$$

with the following properties: if $\mathcal{T}_3 \to \mathcal{T}_2$ (resp., $\mathcal{T}_2 \to \mathcal{T}_0$) is a 3–2 (resp., 2–0) Pachner move of 1-efficient triangulations, there exist maps $\phi_{3,2}$ and $\phi_{2,0}$ that fit in the commutative

diagrams

$$
\begin{array}{ccc}
 & \widehat{\mathcal{G}}^{\mathrm{ev}}(\mathcal{T}_2) & \\
\overset{\widehat{\mathrm{tr}}_{\mathcal{T}_2}}{\nearrow} & \downarrow \phi_{3,2} \overset{I_{\mathcal{T}_2}}{\searrow} & \\
\mathcal{S}^{\mathrm{ev}}(M) & & \mathbb{Z}(\!(q^{1/2})\!) \\
\underset{\widehat{\mathrm{tr}}_{\mathcal{T}_3}}{\searrow} & \widehat{\mathcal{G}}^{\mathrm{ev}}(\mathcal{T}_3) \underset{I_{\mathcal{T}_3}}{\nearrow} &
\end{array}
\qquad
\begin{array}{ccc}
 & \widehat{\mathcal{G}}^{\mathrm{ev}}(\mathcal{T}_0) & \\
\overset{\widehat{\mathrm{tr}}_{\mathcal{T}_0}}{\nearrow} & \downarrow \phi_{2,0} \overset{I_{\mathcal{T}_0}}{\searrow} & \\
\mathcal{S}^{\mathrm{ev}}(M) & & \mathbb{Z}(\!(q^{1/2})\!) \\
\underset{\widehat{\mathrm{tr}}_{\mathcal{T}_2}}{\searrow} & \widehat{\mathcal{G}}^{\mathrm{ev}}(\mathcal{T}_2) \underset{I_{\mathcal{T}_2}}{\nearrow} &
\end{array}
\qquad (5)
$$

To apply the above theorem and define that map I_M, we need a canonical island of 1-efficient triangulations that are connected by 2–0 and 3–2 Pachner moves. Such an island exists for cusped hyperbolic 3-manifolds M, and the corresponding triangulations are obtained from regular subdivisions of the canonical ideal cell decomposition of M, after possibly adding tetrahedra to triangulate the faces of the ideal cells. This is discussed in detail in [GHRS15, Sec.6]. This and Theorem 1.2 implies that for any 1-efficient triangulation $\mathcal{T}$ in that island, the composition

$$
\mathcal{S}^{\mathrm{ev}}(M) \xrightarrow{\widehat{\mathrm{tr}}_{\mathcal{T}}} \widehat{\mathcal{G}}^{\mathrm{ev}}(\mathcal{T}) \xrightarrow{I_{\mathcal{T}}} \mathbb{Z}(\!(q^{1/2})\!) \tag{6}
$$

is independent of $\mathcal{T}$ and defines the map I_M of Theorem 1.1.

We end this introduction with some remarks on the map (2).

Remark 1.3. The image V_M^{3d} of the map (2) (and consequently, of the map (4)) after tensoring with $\mathbb{Q}$ is a $\mathbb{Q}[q^{\pm 1/2}]$-module of finite rank. This follows from the fact that the defining formula for the 3d-index is a proper q-hypergeometric sum, and hence q-holonomic; see [WZ92] and also [GL16]. On the other hand, it is not known that the quantum gluing module $\widehat{\mathcal{G}}^{\mathrm{ev}}(\mathcal{T})$ has finite rank over $\mathbb{Q}(q^{1/2})$. The rank of V_M^{3d} should be related to the rank of the $\mathrm{SL}_2(\mathbb{C})$-Floer Homology defined by Côté–Manolescu [CM19] as well as on the size r of the matrices that appear in the holomorphic quantum modular forms of knot complements [GZ, GZ23].

Remark 1.4. The power series in $q^{1/2}$ that appear in the image of the map (2) are not only convergent for $|q| < 1$, but also (as is lesser known) for $|q| > 1$; see Remark 5.1. Their asymptotic expansions as q approaches a root of unity is related to the asymptotic expansion of perturbative complex Chern–Simons theory and was studied in detail in [GZ23].

Remark 1.5. Much like the DGG 3d-index, the map $I_{\mathcal{T}}$ is effectively computable, and in fact it has been computed before it was defined for the complement of the three simplest hyperbolic knots, namely the 4_1, 5_2 and $(-2, 3, 7)$-pretzel knot in [DGG]. Examples of computation are included in Section 6.

2. Skein modules

In this section we review the basic properties of the skein module and its local version (i.e., the stated skein module) and its variants. Note $q^{1/2}$ in [GY] is $q^{1/8}$ here.

2.1. Kauffman bracket skein modules.

Let M be an oriented 3-manifold, possibly with boundary. The *Kauffman bracket skein module*, denoted by $\mathcal{S}(M)$, is the $\mathbb{Z}[\mathbf{i}][q^{\pm 1/8}]$-module spanned by unoriented framed links in M modulo the following skein relations.

$$\diagup\!\!\!\!\diagdown = q^{1/4}\,\big)\big(+ q^{-1/4}\,\asymp, \qquad \bigcirc = (-q^{1/2} - q^{-1/2})\,\;\;. \tag{7}$$

Here, each diagram is a portion of the link inside a 3-ball with vertical framing, and the parts of the links outside the diagrams are the same in each equation.

By inspection, the homology class of the links in $H = H_1(M; \mathbb{Z}/2)$ is unchanged by the defining relations. Thus, $\mathcal{S}(M)$ is H-graded.

Given a surface, the skein algebra $\mathcal{S}(\Sigma)$ is defined as $\mathcal{S}(\Sigma \times [-1, 1])$ with the product given by stacking. Our convention is $\alpha \cup \beta$ stacks α above β.

We can use a surface to describe a 3-manifold by choosing a Heegaard surface $i : \Sigma \hookrightarrow M$. In other words, M can be recovered by attaching 2- and 3-handles to $\Sigma \times [-1, 1]$. By [Prz99, Proposition 2.2], the natural map $i_* : \mathcal{S}(\Sigma) \to \mathcal{S}(M)$ is surjective, and the kernel is generated by handle slides. In addition, the map i_* behaves as expected on the homology gradings.

2.2. Stated skein algebras.

We recall the stated skein algebras defined by Lê [Lê18]. A *punctured bordered surface* is a surface of the form $\Sigma = \overline{\Sigma} \setminus \mathcal{P}$, where $\overline{\Sigma}$ is a compact oriented surface, possibly with boundary, and $\mathcal{P}$ is a finite set that intersects every component of $\partial\overline{\Sigma}$. A component of $\partial\Sigma$ is called a *boundary edge*, which is homeomorphic to an open interval.

A *tangle* over Σ is an unoriented embedded 1-dimensional submanifold $\alpha \subset \Sigma \times [-1, 1]$ such that $\partial\alpha$ is in $\partial\Sigma \times [-1, 1]$, and that the heights (i.e. the second coordinates) of $\partial\alpha$ are distinct over each boundary edge.

A *framing* of a tangle α over Σ is a transverse vector field along α which is vertical at $\partial\alpha$. Here, *vertical* means tangent to $\{*\} \times [-1, 1]$ in the positive direction. A *state* of a tangle α is a map $\partial\alpha \to \{+, -\}$. By convention, $\pm$ are identified with ± 1 when necessary. Throughout the paper, all tangles will be framed and stated. An *isotopy* of tangles over Σ is homotopy within the class of tangles over Σ. In particular, the height order of $\partial\alpha$ over each boundary edge of Σ is preserved by isotopy.

The *stated skein module* $\mathcal{S}(\Sigma)$ is the $\mathbb{Z}[\mathbf{i}][q^{\pm 1/8}]$-module spanned by stated and framed tangles satisfying the skein relations (7) and following boundary relations.

$$\overline{\subset}^{\,+}_{\,-} = q^{-1/8}\;\;\Big|, \qquad \overline{\subset}^{\,-}_{\,+} = -q^{-5/8}\;\;\Big|, \qquad \overline{\subset}^{\,+}_{\,+} = \overline{\subset}^{\,-}_{\,-} = 0, \tag{8}$$

$$\supset\uparrow = q^{1/8}\;\underline{\quad}^{\,-}_{\,+} - q^{5/8}\;\underline{\quad}^{\,+}_{\,-}. \tag{9}$$

The same diagram conventions as before apply here. In addition, an arrow on the boundary of the surface indicates that as one follows the direction of the arrow, the heights of the endpoints are consecutive and increasing. Although the arrows here follow the induced orientation on the boundary, an isotopy of the tangle can reverse it. For example,

$$\diagup\!\!\!\!\diagdown^{\,\mu}_{\,\nu} = \underline{\quad}^{\,\nu}_{\,\mu}. \tag{10}$$

The homology grading from the last section generalizes to the stated skein algebra using the relative homology $H_1(\Sigma, \partial\Sigma; \mathbb{Z}/2)$. The stated skein algebra has an additional $\mathbb{Z}$-grading d_e on each bound edge e by the sum of states.

Although $\mathcal{S}(\Sigma)$ has a stacking product $\cup$ as before, for the special class of surfaces we consider, there is a necessary modification.

A *boundary triangle* of a punctured bordered surface Σ is a boundary component of $\overline{\Sigma}$ containing 3 boundary edges, and a *surface with triangular boundary* is a punctured bordered surface Σ with a distinguished set of boundary triangles.

Suppose Σ with triangular boundary, we define a new product structure on $\mathcal{S}(\Sigma)$, which we denote by $\cdot$. It is modified from $\cup$ by a power of q. The reason for this modification is to obtain the correct quantization in Section 3.3. Without stating otherwise, we use $\cdot$ as the product for the rest of the paper.

Let $\omega : \mathbb{Z}^3 \otimes \mathbb{Z}^3 \to \mathbb{Z}$ be the skew-symmetric bilinear form with the matrix

$$\begin{pmatrix} 0 & 1 & -1 \\ -1 & 0 & 1 \\ 1 & -1 & 0 \end{pmatrix} \tag{11}$$

For each boundary triangle $E = \{e_1, e_2, e_3\}$, label the edges cyclically as Figure 1. Then the gradings of a tangle α form a vector $d_E(\alpha) = (d_{e_1}(\alpha), d_{e_2}(\alpha), d_{e_3}(\alpha)) \in \mathbb{Z}^3$. For tangles α, β, define a new product by

$$\alpha \cdot \beta = q^{-\frac{1}{8} \sum_E \omega(d_E(\alpha), d_E(\beta))} \alpha \cup \beta \tag{12}$$

where the sum is over all boundary triangles E. It is easy to see that this extends linearly to an associative product with the empty tangle as unit.
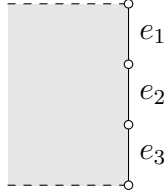

FIGURE 1. Cyclic labeling of the boundary edges in a boundary triangle.

2.3. **Corner reduction and splitting homomorphism.** We want to split surfaces into elementary pieces. In the case of punctured bordered surface, the relation (9) introduced by Lê in [Lê18] is key to make splitting along ideal arcs work. Similarly, we introduced corner reduction in [GY] to make splitting along closed curves work.

Suppose Σ is a surface with triangular boundary. The *corner-reduced skein module* $\mathcal{S}_{\mathrm{cr}}(\Sigma)$ is the quotient of $\mathcal{S}(\Sigma)$ by the left ideal (using $\cdot$ product) generated by the following relations near the boundary triangles.

$$\begin{array}{cccc} \reflectbox{C}\!{}^-_+ = 0, & \reflectbox{C}\!{}^-_- = -\mathbf{i}q^{-1/4}, & \reflectbox{C}\!{}^+_+ = \mathbf{i}q^{1/4}, & \reflectbox{C}\!{}^+_- = 1. \end{array} \tag{13}$$

Note these relations do not preserve the homology or the state sum gradings.

We say a local relation holds at the bottom if it remains true after adding strands above the one shown. This is slightly stronger than a left ideal since the additional strands are allowed connect to the existing ones outside the local picture.

Lemma 2.1 ([GY, Corollary 4.13, Lemma 4.14]). *In $\mathcal{S}_{\mathrm{cr}}(\Sigma)$, the following relations hold at the bottom near boundary triangles.*

$$\overset{\frown}{\bigcirc} = \bigcirc \smile . \tag{14}$$

$$\underline{\quad}\Big|_{+} = \mathbf{i}q^{\frac{1}{8}(d-d'+3)} \diagup\Big|^{-} , \qquad \underline{\quad}\Big|_{-} = \mathbf{i}q^{\frac{1}{8}(d'-d+3)} \diagup\Big|^{+} + q^{\frac{1}{8}(2d''-d-d'+1)} \diagup\Big|^{-} . \tag{15}$$

$$\diagup\Big|^{-} = -\mathbf{i}q^{\frac{1}{8}(d'-d-3)} \underline{\quad}\Big|_{+} , \qquad \diagup\Big|^{+} = q^{\frac{1}{8}(2d''-d-d'-1)} \underline{\quad}\Big|_{+} - \mathbf{i}q^{\frac{1}{8}(d-d'-3)} \underline{\quad}\Big|_{-} . \tag{16}$$

Here, d and d' are the gradings of the left-hand sides on the top and bottom edges, respectively, and d'' is the grading on the third edge in the same boundary triangle (not shown in the diagrams).

Let Σ be a surface with triangular boundary. Given a closed curve c in the interior of the surface and 3 distinguished points p_1, p_2, p_3 on c, we can remove the 3 points from Σ and split Σ along c to obtain a new surface Σ_c with triangular boundary. Let $p : \Sigma_c \to \Sigma$ be the gluing map.

Let α be a tangle diagram on Σ. We can isotope α to be disjoint from the points p_i and transverse to the curve c. If we simply split the diagram, then the new boundary edges are missing height orders and states. To resolve the height, we choose an orientation for each arc between the points p_i on c, and use the lift of the orientation as the height orders for Σ_c. The states are simply summed.

$$\Theta_c(\alpha) = \sum_{s:\alpha\cap c\to\{\pm\}} (\alpha, s). \tag{17}$$

Here, (α, s) means for each $x \in \alpha \cap c$, we assign $s(x)$ to the two endpoints of the split diagram in $p^{-1}(x)$. As an example,

$$\Theta_c\left(\begin{array}{c} p_2 \\ \hline \\ \hline \\ p_1 \end{array} \right) = \sum_{\mu,\nu=\pm} \begin{array}{c} \\ \overset{\mu}{\underset{\nu}{\Big|}}\,\overset{\mu}{\underset{\nu}{\Big|}} \\ \end{array} . \tag{18}$$

Theorem 2.2 ([GY, Theorem 4.16]). Θ_c *is a well-defined homomorphism* $\mathcal{S}_{\mathrm{cr}}(\Sigma) \to \mathcal{S}_{\mathrm{cr}}(\Sigma_c)$.

Note when $\Sigma_c = \Sigma_1 \sqcup \Sigma_2$ is disconnected, $\mathcal{S}_{\mathrm{cr}}(\Sigma_c)$ naturally splits as a tensor product, so the splitting homomorphism takes the form

$$\mathcal{S}_{\mathrm{cr}}(\Sigma) \to \mathcal{S}_{\mathrm{cr}}(\Sigma_1) \otimes \mathcal{S}_{\mathrm{cr}}(\Sigma_2). \tag{19}$$

2.4. **Coalgebra of the annulus.** In addition to being able to split a surface into elementary pieces, another important use of splitting is to localize complex calculations. Let $\mathbb{A}$ denote the annulus with 3 punctures on both boundary components, so $\mathbb{A}$ has triangular boundary. Choose a simple arc from one side to the other as the standard arc. When $\mathbb{A}$ is split

along its core, both components are identified with $\mathbb{A}$ using the standard arc. This splitting homomorphism defines a comultiplication

$$\Delta : \mathcal{S}_{\mathrm{cr}}(\mathbb{A}) \to \mathcal{S}_{\mathrm{cr}}(\mathbb{A}) \otimes \mathcal{S}_{\mathrm{cr}}(\mathbb{A}). \tag{20}$$

Suppose Σ is a surface with triangular boundary. Then similarly, the splitting homomorphism along a curve parallel to a boundary triangle makes $\mathcal{S}_{\mathrm{cr}}(\Sigma)$ a $\mathcal{S}_{\mathrm{cr}}(\mathbb{A})$-comodule.

This is useful because $\mathcal{S}_{\mathrm{cr}}(\mathbb{A})$ also has a counit

$$\epsilon : \mathcal{S}_{\mathrm{cr}}(\mathbb{A}) \to \mathbb{Z}[\mathbf{i}][q^{\pm 1/8}] \tag{21}$$

by [GY, Corollary 4.19]. This implies that the coaction followed by the counit is identity. In particular, we can isotope the complicated part of a diagram on Σ in a neighborhood of a boundary triangle and simplify the diagram using this strategy. To describe the counit, we use [GY, Theorem 4.18], which shows that there is a spanning set consisting of diagrams that are parallel copies of the standard arc with some fixed height orders. For the diagram α in Figure 2,

$$\epsilon(\alpha) = \begin{cases} 1, & \mu_i = \nu_i \text{ for all } i, \\ 0, & \text{otherwise.} \end{cases} \tag{22}$$

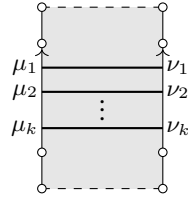Note it is crucial that the arrows are parallel in Figure 2.

FIGURE 2. Diagram α in the annulus $\mathbb{A}$.

2.5. Even skein modules.

In this section we recall the properties of the even skein modules. As before, we fix a compact oriented 3-manifold M. The skein module $\mathcal{S}(M)$ is graded by the homology $H_1(M; \mathbb{Z}/2)$. The degree 0 part is a version of the even skein module, but by this definition, the coefficients are still in $\mathbb{Z}[\mathbf{i}][q^{\pm 1/8}]$, same as $\mathcal{S}(M)$. We can arrange the coefficients to be in $\mathbb{Z}[q^{\pm 1/2}]$ by introducing more grading restrictions.

As a $\mathbb{Z}[q^{\pm 1/2}]$-module, $\mathbb{Z}[\mathbf{i}][q^{\pm 1/8}]$ has a $(\mathbb{Z}/2 \times \mathbb{Z}/4)$-grading using powers of $\mathbf{i}$ and $q^{1/8}$. This makes $\mathbb{Z}[q^{\pm 1/2}]$ the degree 0 part of $\mathbb{Z}[\mathbf{i}][q^{\pm 1/8}]$. We identify the counterpart of this grading on framed links.

Note the defining relations (7) do not have $\mathbf{i}$ or $q^{1/8}$, so we only need to take care of $q^{1/4}$. This is solved by the framing, since a Reidemeister I move (adding a full twist in framing) results in a factor of $-q^{\pm 3/4}$. [Bar99] describes a $\mathbb{Z}/2$ assignment $\Sigma\mathrm{Spin}$, abbreviated here by σ, to framed links depending on a spin structure on M. In particular, Seifert framed knots in a ball have $\sigma = 0$. When restricted to links with even homology, σ is independent of the spin structure as well. Thus, we can define the $(\mathbf{i}, q^{1/8})$-degree of a framed link as $(0, 2\sigma)$. Then the even skein module $\mathcal{S}^{\mathrm{ev}}(M)$ is defined as the $\mathbb{Z}[q^{\pm 1/2}]$-submodule where all gradings are zero, and (7) can be restricted to $\mathcal{S}^{\mathrm{ev}}(M)$ by [Bar99].

Now suppose Σ is a punctured bordered surface. The even skein algebra $\mathcal{S}^{\mathrm{ev}}(\Sigma)$ similarly requires zero homology class in $H_1(\Sigma, \partial\Sigma; \mathbb{Z}/2)$, but we also need to describe framing and state requirements for tangles. Let α be a tangle over Σ with even homology. Then on each boundary edge, the number of endpoints is even. By an isotopy, we require the diagram near the boundary edge have positive height order, i.e. like the order in the defining relation (9). We can pair up the endpoints and connect like (9) without introducing new crossings. Let $\bar{\alpha}$ be a link obtained this way. Then we define $\sigma(\alpha) = \sigma(\bar{\alpha})$. Again using the argument of [Bar99], $\sigma(\alpha)$ is independent of how $\bar{\alpha}$ is connected. Define two more quantities: $2n(\alpha)$ is the number of endpoints of α, and $2d(\alpha)$ is the sum of all states of α. n and d are both integers when α has even homology. Now define the $(\mathbf{i}, q^{1/8})$-degree of α as $(d(\alpha), 2\sigma(\alpha) - n(\alpha))$. Then the even skein algebra $\mathcal{S}^{\mathrm{ev}}(\Sigma)$ is again defined as the $\mathbb{Z}[q^{\pm 1/2}]$-submodule where all gradings are zero. More explicitly,

$$\mathcal{S}^{\mathrm{ev}}(\Sigma) = \mathrm{Span}_{\mathbb{Z}[q^{\pm 1/2}]}\{\mathbf{i}^{d(\alpha)}q^{n(\alpha)/8+\sigma(\alpha)/4}\alpha \mid \alpha \text{ has even homology}\}. \qquad (23)$$

It is easy to check that the defining relations (7)–(9) restricts to $\mathcal{S}^{\mathrm{ev}}(M)$.

If Σ is a dual surface of the 3-manifold M, then the natural map $\mathcal{S}(\Sigma) \twoheadrightarrow \mathcal{S}(M)$ is still surjective on the even part $\mathcal{S}^{\mathrm{ev}}$. Although the Σ-diagram of an even link in M may not have even homology, the difference in homology is generated by A, B-circles, so handle slides bring the diagram to even.

Finally, we deal with the corner reduction. Since the gradings above do not easily descend to $\mathcal{S}_{\mathrm{cr}}(\Sigma)$, we define the even part $\mathcal{S}_{\mathrm{cr}}^{\mathrm{ev}}(\Sigma)$ simply as the image of $\mathcal{S}^{\mathrm{ev}}(\Sigma)$ in the quotient $\mathcal{S}(\Sigma) \twoheadrightarrow \mathcal{S}_{\mathrm{cr}}(\Sigma)$.

Lemma 2.3. Let Σ_c be Σ split along a closed curve c. Then the image of $\mathcal{S}_{\mathrm{cr}}^{\mathrm{ev}}(\Sigma)$ under the splitting $\mathcal{S}_{\mathrm{cr}}(\Sigma) \to \mathcal{S}_{\mathrm{cr}}(\Sigma_c)$ is in the even part $\mathcal{S}_{\mathrm{cr}}^{\mathrm{ev}}(\Sigma_c)$.

Proof. Recall 3 points are removed from c to make Σ_c. Let Σ' be Σ minus these 3 points. Then Σ_c is Σ' split along 3 ideal arcs. By the same handle slide argument as above, a tangle with even homology can be isotoped so that it is even on Σ'. Then it is easy to see that the split diagram has even homology on Σ_c.

Next we consider the $\mathbf{i}$-degree d. By definition, the change in d after splitting comes from the extra states created by the splitting. However, the matching states of splitting and the even intersection with c shows that the change in d is even.

Finally, we deal with the $q^{1/8}$-degree $2\sigma - n$. When done with diagrams, the height order on each pair of new boundary edges have opposite orientations. See (18). This means an isotopy is required to twist the side with negative order to positive. After pairing the endpoints and connecting them, the twist from the negative side becomes a Reidemeister I move for each pair of endpoints, as shown in the following example.

$$(24)$$

Thus, the change in the framing and the number of endpoints cancel to preserve the $q^{1/8}$ degree. □

Lemma 2.4. $\mathcal{S}_{\mathrm{cr}}^{\mathrm{ev}}(\mathbb{A})$ is the $\mathbb{Z}[q^{\pm 1/2}]$-span of diagrams of the form Figure 2 with even number of components. As a result, the image of $\mathcal{S}_{\mathrm{cr}}^{\mathrm{ev}}(\mathbb{A})$ under the counit $\epsilon : \mathcal{S}_{\mathrm{cr}}(\mathbb{A}) \to \mathbb{Z}[\mathbf{i}][q^{\pm 1/8}]$ is $\mathbb{Z}[q^{\pm 1/2}]$.

Proof. The second part follows from the first since the counit of Figure 2 is 0 or 1, so we focus on the first part.

[GY, Appendix A] described how to reduce tangle diagrams on $\mathbb{A}$. By applying the defining relations (7)–(9) and the relations from Lemma 2.1 in a specific direction, any diagram can be reduced to the form in Figure 2. As mentioned before, the defining relations preserve all gradings as mentioned before.

The rest of the relations change the homology, but the evenness of the original diagram implies that if any of them applies to the diagram, then another relation of the same type also applies immediately afterwards. Therefore, we can combine these relations in a way the preserves the homology class. After careful calculations with the coefficients, we see that the combinations also preserve all gradings. Here we give one example.

$$\text{(25)}$$

The height order is positive throughout, and the relations hold at the bottom. The meaning of d, d' is the same as in Lemma 2.1. The coefficient combines into $-q^{\frac{1}{8}(2d'-2d-6)}$, which compensates the framing change introduced by the crossing. The $\mathbf{i}$-grading also changes by $+2$, which is even.

Therefore, there is a set of reduction rules that preserve all gradings, and any even diagram is reduced to the form in Figure 2. This proves the lemma. $\qquad\square$

3. QUANTUM TRACE MAP

As mentioned in the introduction, the 3d-quantum trace map plays a key role in the proof of Theorems 1.1 and 1.2. In this section we review its definition and its properties following the notation of our previous work [GY].

3.1. **Dual surface from triangulation.** Let T be an oriented tetrahedron. A labeling of the vertices of T by $0, 1, 2, 3$ is compatible with the orientation if vertices $1, 2, 3$ are counterclockwise when viewed from vertex 0. The tetrahedron has a dual surface $\mathbb{L}$ which is a sphere with 4 boundary components. Borrowing from the theory of mapping class groups of surfaces, we call it the *lantern*. The boundary circles of the lantern are labeled according to the vertex opposite to it. The lantern also comes with 6 *standard arcs* dual to the edges of T. The embedding of the lantern and a top view are given in the first two parts of Figure 3, where the blue arcs are the standard arcs. The last part is the lantern laid flat in the plane. Note the reordering of the labels to maintain the orientation.

Suppose M is a compact oriented 3-manifold possibly with boundary. Given a collection of tetrahedra $\mathcal{T} = \{T_1, \ldots, T_N\}$ and orientation reversing face pairing, if the space obtained from gluing the tetrahedra minus the vertices is homeomorphic to the interior of M preserving the orientation, then $\mathcal{T}$ is an oriented triangulation of M.
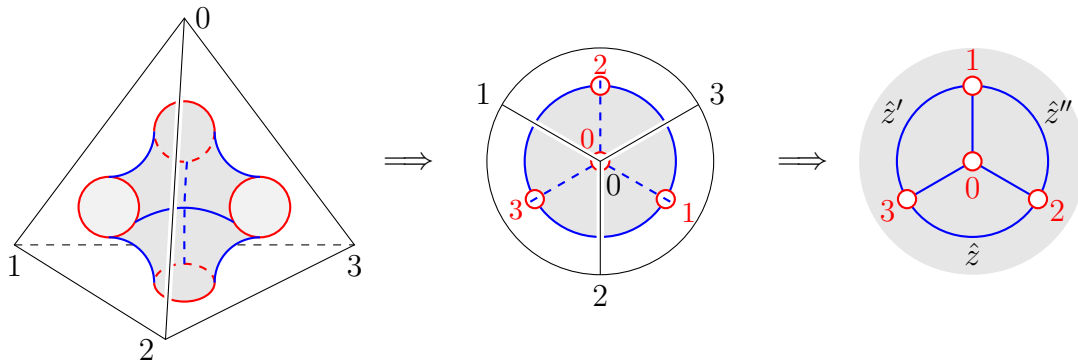
FIGURE 3. Lantern surface in a tetrahedron.

Given an ideal triangulation $\mathcal{T}$, there is an embedded (Heegaard) surface $\Sigma_{\mathcal{T}} \subset M$ glued from the lanterns in the tetrahedra. The standard arcs around the same edge e in the triangulation are connected to form a curve B_e when the lanterns are glued. On the other hand, each face f of the triangulation contains a circle A_f which is a boundary circle of the adjacent lantern. The data $\mathcal{H}_{\mathcal{T}} := (\Sigma_{\mathcal{T}}, \{A_f\}, \{B_e\})$ is called the *dual surface* of $\mathcal{T}$. It is equivalent to the triangulation $\mathcal{T}$ since the intersection pattern of the curves $\{A_f\}$ and $\{B_e\}$ determines the face pairings of the triangulation. Also note that M can be obtained directly from $\mathcal{H}_{\mathcal{T}}$. This can be done by gluing 2-handles to $\Sigma_{\mathcal{T}} \times [-1, 1]$ along $A_f \times \{-1\}$ and $B_e \times \{1\}$ and then capping off spherical boundary components as necessary. Note the A-circles determine the handlebody inside the dual surface.

3.2. **Quantum tori.** Let us briefly recall this notion of Laurent polynomials in q-commuting variables. A quantum torus on generators $x_1, \ldots, x_r$ over an algebra R is an associative R-algebra with unit of the form

$$\mathbb{T}\langle x_1, \ldots, x_r \rangle := R\langle x_1^{\pm 1}, \ldots, x_r^{\pm 1} \rangle / \langle x_i x_j - q^{D_{ij}} x_j x_i \rangle \qquad (26)$$

for some skew-symmetric $r \times r$ matrix D. It is a free R-module with basis

$$[\vec{x}^k] = q^{-\frac{1}{2} \sum_{i<j} D_{ij} k_i k_j} x_1^{k_1} \cdots x_r^{k_r}, \qquad k = (k_1, \ldots, k_r) \in \mathbb{Z}^r. \qquad (27)$$

These monomials are called *Weyl-ordered*, which is designed to be independent of the order of the generators. This normalization can be formally understood as the Baker-Campbell-Hausdorff formula for $e^{\sum_i k_i \ln(x_i)}$. Note that Weyl-ordering can be defined for all products with q-commuting factors.

The product on the quantum torus can be described using the Weyl-ordered monomial basis as

$$[\vec{x}^k][\vec{x}^l] = q^{\frac{1}{2}\omega(k,l)}[x^{k+l}] = q^{\omega(k,l)} x^l x^k, \qquad (28)$$

where $\omega(k, l) = k^t D l$ is the bilinear form associated to D.

3.3. **Quantum gluing module.** We next recall the quantum gluing module associated to an ideal triangulation. First consider a single tetrahedron. The quantum gluing module $\widehat{\mathcal{G}}(\mathbb{L})$ is a quotient of the quantum torus over $\mathbb{Z}[\mathbf{i}][q^{\pm 1/8}]$

$$\widehat{\mathcal{G}}(\mathbb{L}) = \mathbb{T}\langle \hat{z}, \hat{z}', \hat{z}'' \rangle /_L \langle \hat{z}^{-2} + \hat{z}''^2 - 1, [\hat{z}\hat{z}'\hat{z}''] - \mathbf{i}q^{1/4} \rangle, \qquad (29)$$

where the q-commuting relations are given by $\frac{1}{4}\omega$ from (11). Explicitly,

$$\hat{z}\hat{z}' = q^{1/4}\hat{z}'\hat{z}, \qquad \hat{z}'\hat{z}'' = q^{1/4}\hat{z}''\hat{z}, \qquad \hat{z}''\hat{z} = q^{1/4}\hat{z}\hat{z}''. \tag{30}$$

Note that $[\hat{z}\hat{z}'\hat{z}'']$ is central, so we can eliminate one of the generators, typically $\hat{z}'$, from the quantum torus. We will freely do so when convenient.

The variables $\hat{z}, \hat{z}', \hat{z}''$ correspond to the 01, 02, 03 edges, respectively, and opposite edges are assigned the same generators. It is easy to check that orientation preserving symmetries of $\widehat{\mathcal{G}}(\mathbb{L})$ induce cyclic permutations of $\hat{z}, \hat{z}', \hat{z}''$ so the definition is independent of the labeling of the tetrahedron.

Remark 3.1. In [GY], $\widehat{\mathcal{G}}(\mathbb{L})$ has an extra generator $\hat{y}$ satisfying $\hat{y}^2 = \hat{z}^2$. In our main consideration of 3d-index, only squares appear, so the distinction is irrelevant.

Let $\mathcal{T}$ be an oriented triangulation of an oriented 3-manifold M with torus boundary. Throughout, N is the number of tetrahedra, r is the number of boundary components, i index edges, j index tetrahedra. In the notations of the ideal, the range of indices are omitted when clear from context.

The quantum gluing module $\widehat{\mathcal{G}}(\mathcal{T})$ is defined as

$$\widehat{\mathcal{G}}(\mathcal{T}) := \langle \hat{e}_i + q^{1/2} \rangle_R \backslash \Big(\bigotimes_{j=1}^{N} \mathbb{T}\langle \hat{z}_j, \hat{z}_j'' \rangle \Big) /_L \langle \hat{z}_j^{-2} + \hat{z}_j''^2 - 1 \rangle, \tag{31}$$

where $\hat{e}_i$ is the Weyl-ordered product of $\hat{z}_j^{\square}$ around the i-th edge. The monomials $\hat{e}_i$ commute with each other by [Neu92, Theorem 4.1]. Moreover, $N - r$ of them, say $\hat{e}_1, \ldots, \hat{e}_{N-r}$, are independent, and the rest can be written as monomials in $\hat{e}_1, \ldots, \hat{e}_{N-r}$. The argument of [GHRS15, Remark 4.6] shows that the independent $N - r$ edges also generate the same right ideal.

3.4. Quantum trace map. The quantum trace map

$$\widehat{\mathrm{tr}}_{\mathcal{T}} : \mathcal{S}(M) \to \widehat{\mathcal{G}}(\mathcal{T}) \tag{32}$$

is defined by the following diagram:

$$
\begin{array}{ccccc}
\mathcal{S}(\Sigma_{\mathcal{T}}) & \xrightarrow{\Theta_A} & \bigotimes_{j=1}^{N} \mathcal{S}_{\mathrm{cr}}(\mathbb{L}_j) & \longrightarrow & \bigotimes_{j=1}^{N} \widehat{\mathcal{G}}(\mathbb{L}_j) \\
\downarrow & & & & \downarrow \\
\mathcal{S}(M) & \dashrightarrow{\quad\widehat{\mathrm{tr}}_{\mathcal{T}}\quad} & & & \widehat{\mathcal{G}}(\mathcal{T})
\end{array}
. \tag{33}
$$

Here Θ_A is the splitting map along all A-circles, and $\mathcal{S}_{\mathrm{cr}}(\mathbb{L}) \twoheadrightarrow \widehat{\mathcal{G}}(\mathbb{L})$ sends a standard arc with $-$ states at both endpoints to the corresponding generator $\hat{z}^{\square}$. More generally, the standard arcs with states μ, ν is sent to $\delta_{\mu\nu}(\hat{z}^{\square})^{-\mu}$.

Remark 3.2. Suppose M has a boundary component with Euler characteristic $\chi \neq 0$, then the quantum gluing module $\widehat{\mathcal{G}}(\mathcal{T})$ has quantum inconsistency. There is a product of $\hat{e}_i$ which is 1 in the quantum torus but $q^{\chi/2}$ according to the quotient. Although quantum trace map

is still defined in this case, most applications, such as 3d-index considered in this paper, require consistency. Therefore, we only consider torus boundary in this paper.

3.5. **Even gluing modules.** We now introduce an even version of the quantum gluing module. The even gluing module $\widehat{\mathcal{G}}^{\mathrm{ev}}(\mathcal{T})$ is defined as the $\mathbb{Z}[q^{\pm 1/2}]$-span of squares of Weyl-ordered monomials. We adopt the convention that an upper case letter is the square of the lower case letter, e.g. $\hat{Z} = \hat{z}^2$. Note the coefficients in the following relations are in $\mathbb{Z}[q^{\pm 1/2}]$.

$$\hat{Z}''\hat{Z} = q^{1/2}[\hat{Z}\hat{Z}''] = q\hat{Z}\hat{Z}'', \qquad [\hat{Z}\hat{Z}'\hat{Z}''] = -q^{1/2}. \tag{34}$$

Let $\mathbb{T}^{\mathrm{ev}}$ denote a quantum torus over $\mathbb{Z}[q^{\pm 1/2}]$. Then $\widehat{\mathcal{G}}^{\mathrm{ev}}(\mathcal{T})$ is a quotient of $\bigotimes_j \mathbb{T}^{\mathrm{ev}}\langle \hat{Z}_j, \hat{Z}_j'' \rangle$. Our goal is to find a presentation based on this quotient.

Recall $\hat{e}_i$ commute with each other, and they generate a lattice Λ of rank $N - r$ (with multiplication as the group operation). Λ can be embedded in $\mathbb{Z}^{2N}$ by taking exponents after eliminating $\hat{z}_j'$ using the vertex equation. This is the same as taking the rows of the Neumann–Zagier matrix.

Lemma 3.3. Suppose M has no non-peripheral $\mathbb{Z}/2$-homology. Then there exists a generating set of monomials $x_1, \ldots, x_{2N} \in \bigotimes_{j=1}^N \mathbb{T}\langle \hat{z}_j, \hat{z}_j'' \rangle$ such that $x_1, \ldots, x_{N-r}$ is an independent subset of $\hat{e}_1, \ldots, \hat{e}_N$.

Proof. $\mathbb{Z}^{2N}$ has a symplectic form that corresponds to the q-commuting relations of $\hat{z}_j, \hat{z}_j''$. By [Neu92, Theorem 4.2], $\Lambda^\perp = \Lambda$ when M has no non-peripheral $\mathbb{Z}/2$-homology. Here, the complement is defined using the symplectic form. This shows that Λ is a direct summand of $\mathbb{Z}^{2N}$. Thus, we can make a change of basis so that $x_1, \ldots, x_{N-r}$ is a basis of $\bar{\Lambda}$, and $x_{N-r+1}, \ldots, x_{2N}$ is the rest of the basis of $\mathbb{Z}^{2N}$. The lemma is just a translation of this basis. $\qquad\square$

Proposition 3.4. If M has no non-peripheral $\mathbb{Z}/2$-homology, then the even part has the presentation

$$\widehat{\mathcal{G}}^{\mathrm{ev}}(\mathcal{T}) = \langle \hat{E}_i - q \rangle_R \backslash \Big(\bigotimes_{j=1}^N \mathbb{T}^{\mathrm{ev}}\langle \hat{Z}_j, \hat{Z}_j'' \rangle \Big)/_L \langle \hat{Z}_j^{-1} + \hat{Z}_j'' - 1 \rangle. \tag{35}$$

If necessary, we can restore $\hat{Z}_j'$ in the presentation and add the (central) relation $[\hat{Z}_j\hat{Z}_j'\hat{Z}_j''] + q^{1/2}$.

Proof. For convenience, write $\mathbb{T}_{\mathcal{T}}^{\mathrm{ev}}$ for the tensor quantum torus. We need to show

$$(\langle \hat{e}_i + q^{1/2} \rangle_R + {}_L\langle \hat{z}_j^{-2} + \hat{z}_j''^2 - 1 \rangle) \cap \mathbb{T}_{\mathcal{T}}^{\mathrm{ev}} = \langle \hat{E}_i - q \rangle_R + {}_L\langle \hat{Z}_j^{-1} + \hat{Z}_j'' - 1 \rangle. \tag{36}$$

Using the generators from Lemma 3.3 and the monomial basis of the quantum torus, we can write an element in the left-hand side of (36) as

$$\sum_{i=1}^{N-r} (x_i + q^{1/2}) \sum_{k \in \mathbb{Z}^{2N-r}} c_{ik}\tilde{x}^k + \sum_{j=1}^N \sum_{k \in \mathbb{Z}^{2N-r}} d_{jk}\tilde{x}^k(\hat{z}_j^{-2} + \hat{z}_j''^2 - 1) \in \mathbb{T}_{\mathcal{T}}^{\mathrm{ev}}, \tag{37}$$

where $c_{ik}, d_{jk} \in \mathbb{Z}[\mathbf{i}][q^{\pm 1/8}][x_1, \ldots, x_{N-r}]$, and $\tilde{x}^k = [x_{N-r+1}^{k_1} \cdots x_{2N}^{k_{2N-r}}]$ is the Weyl-ordered monomial. Since the variables $x_{N-r+1}, \ldots, x_{2N}$ only appear in $\tilde{x}^k$ and $\hat{z}_j, \hat{z}_j''$, terms where

$k \notin (2\mathbb{Z})^{2N-r}$ must cancel for this element to be in $\mathbb{T}_{\mathcal{T}}^{\mathrm{ev}}$, so we may restrict the sum to $k \in (2\mathbb{Z})^{2N-r}$. Using long division, we can extract all $x_i + q^{1/2}$ from d_{jk}, so we can assume d_{jk} are constants.

Let $\mathbb{T}_{\mathcal{T}}^2$ be the $\mathbb{Z}[\mathbf{i}][q^{\pm 1/8}]$-span of squares, or $\mathbb{T}_{\mathcal{T}}^2 = \bigoplus_{s=0}^{1} \bigoplus_{t=0}^{3} \mathbf{i}^s q^{t/8} \mathbb{T}_{\mathcal{T}}^{\mathrm{ev}}$. In (37), the second term is in $\mathbb{T}_{\mathcal{T}}^2$ by assumption, so the first term is in $\mathbb{T}_{\mathcal{T}}^2$ as well. This means

$$\sum_{i=1}^{N-r} (x_i + q^{1/2}) c_{ik} \in \mathbb{T}_{\mathcal{T}}^2 \cap \mathbb{Z}[\mathbf{i}][q^{\pm 1/8}][x_1, \ldots, x_{N-r}] = \mathbb{Z}[\mathbf{i}][q^{\pm 1/8}][x_1^2, \ldots, x_{N-r}^2]. \tag{38}$$

This shows we can rearrange the sum to be $\sum_{i=1}^{N-r} (x_i^2 - q) c'_{ik}$ for $c'_{ik} \in \mathbb{Z}[\mathbf{i}][q^{\pm 1/8}][x_1^2, \ldots, x_{N-r}^2]$. Putting this into (37), we get

$$\sum_{k \in (2\mathbb{Z})^{2N-r}} \Big(\sum_{i=1}^{N-r} (x_i^2 - q) c'_{ik} \tilde{x}^k + \sum_{j=1}^{N} d_{jk} \tilde{x}^k (\hat{z}_j^{-2} + \hat{z}_j''^2 - 1) \Big) \in \mathbb{T}_{\mathcal{T}}^{\mathrm{ev}} \subset \mathbb{T}_{\mathcal{T}}^2. \tag{39}$$

Finally, the $(\mathbb{Z}/2 \times \mathbb{Z}/4)$-grading over $\mathbb{Z}[q^{\pm 1/2}]$ by powers of $\mathbf{i}$ and $q^{1/8}$ can be used to rearrange the coefficients in (39) into $\mathbb{Z}[q^{\pm 1/2}]$. This proves (36). □

Remark 3.5. The same condition on homology appears in [HRS12]. When the condition is not satisfied, it is easy to find extra relations in the even part. We use the example of the hyperbolic census manifold m136 considered in [HRS12]. It has 1 torus boundary and homology $\mathbb{Z} \oplus (\mathbb{Z}/2)^2$, so $H_1(\partial M; \mathbb{Z}/2) \to H_1(M; \mathbb{Z}/2)$ cannot be surjective. Using the default triangulation given by SnapPy with isomorphism signature eLMkbcdddhhqqa, we see there is an edge $\hat{e}_1 = \hat{Z}_1 \hat{Z}_2 \hat{Z}_3 \hat{Z}_4$ already in the even part. This means the even part contains the relation $\hat{e}_1 = -q^{1/2}$, while the naive presentation (35) only contains the weaker condition $\hat{E}_1 = q$. There are refinements of the quantum gluing modules that reduce unexpected evenness but not completely.

This is also reflected in the even skein modules. Suppose Σ is a dual surface of M and consider two even Σ-diagrams for an even link in M. Although they are related by handle slides, the intermediate stages may not be even on Σ. The naive solution is to only slide along curves twice in a row, but when there is non-peripheral $\mathbb{Z}/2$-homology, these moves do not relate all even diagrams. The dual surface to the triangulation above easily produces such an example.

3.6. **The even part of quantum trace.** Having introduced the even skein module and the even gluing module, we now come to the even quantum trace map.

Theorem 3.6. *The quantum trace restricts to a map* $\mathcal{S}^{\mathrm{ev}}(M) \to \widehat{\mathcal{G}}^{\mathrm{ev}}(\mathcal{T})$.

Proof. Since the quantum trace map is induced by $\mathcal{S}(\Sigma) \to \widehat{\mathcal{G}}(\mathcal{T})$, we only need to show that $\mathcal{S}^{\mathrm{ev}}(\Sigma)$ maps to $\widehat{\mathcal{G}}^{\mathrm{ev}}(\mathcal{T})$. By Lemma 2.3, this is further reduced to the statement that $\mathcal{S}_{\mathrm{cr}}(\mathbb{L}) \twoheadrightarrow \widehat{\mathcal{G}}(\mathbb{L})$ maps $\mathcal{S}_{\mathrm{cr}}^{\mathrm{ev}}(\mathbb{L})$ to $\widehat{\mathcal{G}}^{\mathrm{ev}}(\mathbb{L})$.

Choose one of the standard arcs corresponding to $\hat{z}''$. If the lantern is cut along this arc as well as both standard arcs for $\hat{z}$, the result is a disk. Therefore, every diagram on the lantern can be drawn in the neighborhood of these arcs and the boundary triangles. See Figure 4. As explained in [GY, Theorem 4.25], we can draw 4 circles isotopic to the boundary triangles
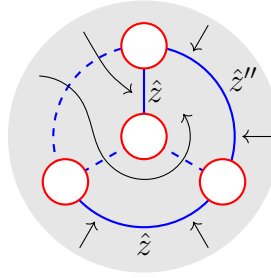
FIGURE 4. Isotopy toward the standard arcs.

such that the diagram consists of standard arcs in the smaller lantern bounded by these curves. We can split along these 4 curves and apply counits, which does not change the element in $\mathcal{S}_{\mathrm{cr}}(\mathbb{L})$. If we start in $\mathcal{S}_{\mathrm{cr}}^{\mathrm{ev}}(\mathbb{L})$, then the counits give coefficients in $\mathbb{Z}[q^{\pm 1/2}]$ by Lemma 2.4, and the standard arcs have even multiplicities by the even homology condition. Therefore, the image in $\widehat{\mathcal{G}}(\mathbb{L})$ is in the even part. □

4. CHANGE OF TRIANGULATION

We want to define maps from the skein module $\mathcal{S}(M)$ that factor through the quantum trace maps for suitable classes of triangulations. This requires an understanding of the relations between quantum trace maps for triangulations related by certain moves. In this paper, we consider the 3–2 and 2–0 moves for the application of 3d-index.
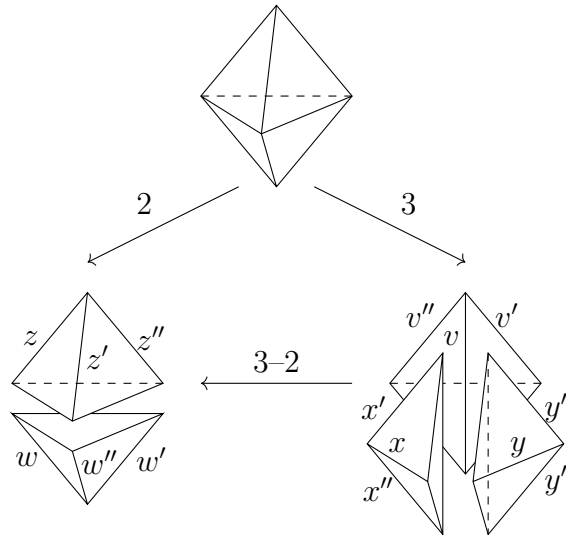

FIGURE 5. 3–2 Pachner move.

4.1. **Compatibility with 3–2 moves.** Suppose $\mathcal{T}_3 \to \mathcal{T}_2$ is a 3–2 move shown in Figure 5. Let $\mathbb{T}_2$ and $\mathbb{T}_3$ be the quantum tori in the definition of $\widehat{\mathcal{G}}(\mathcal{T}_2)$ and $\widehat{\mathcal{G}}(\mathcal{T}_3)$, respectively. Define

$\phi_{3,2} : \mathbb{T}_2 \to \mathbb{T}_3$ by

$$\begin{aligned}
\phi_{3,2}(\hat{z}) = \hat{v}''\hat{x}', &\qquad \phi_{3,2}(\hat{z}') = \hat{x}''\hat{y}', &\qquad \phi_{3,2}(\hat{z}'') = \hat{y}''\hat{v}', \\
\phi_{3,2}(\hat{w}) = \hat{x}''\hat{v}', &\qquad \phi_{3,2}(\hat{w}') = \hat{v}''\hat{y}', &\qquad \phi_{3,2}(\hat{w}'') = \hat{y}''\hat{x}',
\end{aligned} \tag{40}$$

and $\phi_{3,2}$ acts as identity on the remaining generators of $\widehat{\mathcal{G}}(\mathcal{T}_2)$. A straightforward calculation shows that (40) has the correct q-commuting relations, so this is a well-defined algebra map.

Lemma 4.1. The map above induces a well-defined map

$$\phi_{3,2} : \widehat{\mathcal{G}}(\mathcal{T}_2) \to \widehat{\mathcal{G}}(\mathcal{T}_3). \tag{41}$$

Clearly, $\phi_{3,2}$ restricts to a map $\widehat{\mathcal{G}}^{\mathrm{ev}}(\mathcal{T}_2) \to \widehat{\mathcal{G}}^{\mathrm{ev}}(\mathcal{T}_3)$.

Proof. It is easy to see from Figure 5 that the edges $\hat{e}_i \in \mathbb{T}_2$ are mapped to the corresponding monomials in $\mathbb{T}_3$ by $\phi_{3,2}$. It remains to check the Lagrangians are related by $\phi_{3,2}$. For the Lagrangians away from the move region, the statement is trivial, and the cases of $\hat{z}$ and $\hat{w}$ are symmetric. Here, we consider $\hat{z}$.

$$\begin{aligned}
\phi_{3,2}(\hat{z}^{-2} + \hat{z}''^2 - 1) &= (\hat{v}''\hat{x}')^{-2} + (\hat{y}''\hat{v}')^2 - 1 \\
&= \hat{v}''^{-2}(1 - \hat{x}^2 + L_x') + \hat{v}'^2(1 - \hat{y}^{-2} + L_y) - 1 \\
&= (-\hat{v}''^{-2}\hat{v}'^{-2}\hat{x}^2\hat{y}^2 - 1)\hat{v}'^2\hat{y}^{-2} + L_v'' + \hat{v}''^2 L_x' + \hat{v}'^2 L_y \\
&= (q^{-1}\hat{v}^2\hat{x}^2\hat{y}^2 - 1)\hat{v}'^2\hat{y}^{-2} + L_v'' + \hat{v}''^2 L_x' + \hat{v}'^2 L_y.
\end{aligned} \tag{42}$$

Here $L_x' = \hat{x}'^{-2} + \hat{x}^2 - 1$, $L_y = \hat{y}^{-2} + \hat{y}''^2 - 1$, and $L_v'' = \hat{v}''^{-2} + \hat{v}'^2 - 1$ are Lagrangians in $\mathbb{T}_3$. Note $\hat{v}\hat{x}\hat{y} = \hat{e}$ is the extra edge in $\mathbb{T}_3$, which commutes with the image of $\phi_{3,2}$. Then for any $r \in \mathbb{T}_2$,

$$\phi_{3,2}(r(\hat{z}^{-2} + \hat{z}''^2 - 1)) = (q^{-1}\hat{e}^2 - 1)\phi_{3,2}(r)\hat{v}'^2\hat{y}^{-2} + (L_v'' + \hat{v}''^2 L_x' + \hat{v}'^2 L_y). \tag{43}$$

This shows that $\phi_{3,2}(_L\langle \hat{z}^{-2} + \hat{z}''^2 - 1 \rangle) \subset \langle \hat{e} + q^{1/2} \rangle_R + {}_L\langle \text{Lagrangian} \rangle$. $\square$

Proposition 4.2. The quantum trace map is compatible with $\phi_{3,2}$: $\widehat{\mathrm{tr}}_{\mathcal{T}_3} = \phi_{3,2} \circ \widehat{\mathrm{tr}}_{\mathcal{T}_2}$.

Proof. Let $\Sigma_i = \Sigma_{\mathcal{T}_i}$ be the dual surfaces. Away from the move region of Figure 5, the dual surfaces are identical. In the move region, the surfaces are shown in Figure 6. The left figure is Σ_2, and the right figure is Σ_3. A few arcs on Σ_3 are omitted for clarity. The dashed arc in the back of Σ_2 should also be on Σ_3, and the 3 new red arcs should go through the hole of Σ_3 to form complete circles.

To compare the quantum trace maps, we need to know how diagrams on Σ_2 is isotoped onto Σ_3. From Figure 6, it is clear that Σ_2 is obtained from Σ_3 by a surgery along B_e. Given a diagram on Σ_2, an isotopy makes it disjoint from the two disks bounded by the copies of B_e, and reversing the surgery gives a diagram on Σ_3 that defines the same link in M.

Now start with a diagram on Σ_2. By an isotopy, we can assume that the diagram is in a small neighborhood of the standard arcs and the A-circles except the middle one in Figure 6. This is possible since the complement of this neighborhood is disks. We can further assume that near the standard arcs, the diagram is just parallel strands of standard arcs.

First assume that the 6 "boundary" faces of the move region are not paired with each other. The quantum trace requires splitting along A-circles, which creates a sum over states.
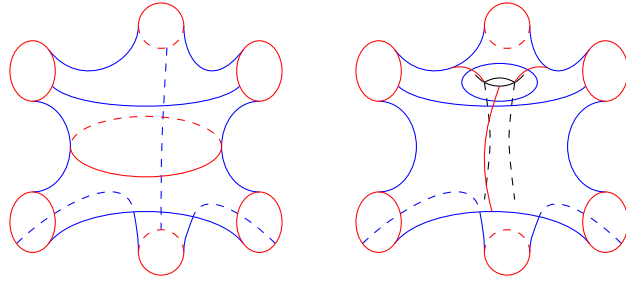
FIGURE 6. Dual surfaces Σ_2 and Σ_3 (a few arcs omitted for clarity).

The sums outside the move region are identical for $\mathcal{T}_2$ and $\mathcal{T}_3$ by assumption, and the sums inside the move region has finitely many cases with 9 types of standard arcs and 4 state combinations each. Then it is straightforward to check that they are given by $\phi_{3,2}$. Here, we only give one calculation as an example. Consider the arc in the back in Figure 6 with $-$ states at both endpoints. On Σ_2, it is split into two standard arcs. The new endpoints must have $-$ states for the diagram to be nonzero in $\widehat{\mathcal{G}}(\mathcal{T}_2)$, in which case it evaluates to $\hat{z}'\hat{w}''$. On Σ_3, it is a single standard arc $\hat{v}$. They are related by $\phi_{3,2}$ since

$$\phi_{3,2}(\hat{z}'\hat{w}'') = (\hat{x}''\hat{y}')(\hat{y}''\hat{x}') = (\mathbf{i}q^{1/4})^2(\hat{x}\hat{y})^{-1} = (-q^{1/2}\hat{e}^{-1})\hat{v} = \hat{v}. \tag{44}$$

As in the proof of Lemma 4.1, $\hat{e} = \hat{x}\hat{y}\hat{v}$ can be set to $-q^{1/2}$ since it commutes with the image of $\phi_{3,2}$. The other arcs are similar.

If there are extra face pairings in the move region, we can double the corresponding A-curves to create a buffer zone, which can be absorbed using the counit of the annulus. The remainder of the argument is the same. $\qquad\square$
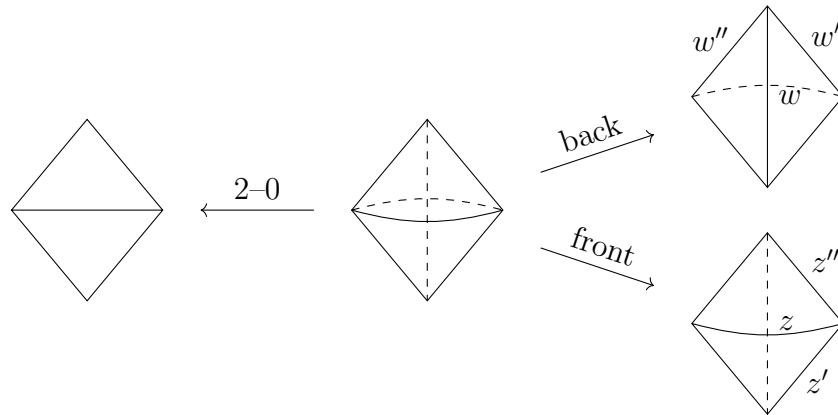

FIGURE 7. 2–0 move.

4.2. **Compatibility with 2–0 moves.** Suppose $\mathcal{T}_2 \to \mathcal{T}_0$ is a 2–0 move. See Figure 7. The construction is similar to the 3–2 move, so less details will be provided.

Remark 4.3. Unlike the 3–2 move, the construction below only works for the even part. This can be traced to the extra quotient mentioned in Remark 3.1. If the full quantum

trace is used, then the 2–0 move will be fully compatible, but a lot more technical details are required. We choose to omit the complete picture to focus on the 3d-index, which only requires the even part.

Suppose M has no non-peripheral $\mathbb{Z}/2$-homology, so presentation (35) is valid. The quantum gluing modules are related by a map

$$\phi_{2,0} : \widehat{\mathcal{G}}^{\mathrm{ev}}(\mathcal{T}_0) \to \widehat{\mathcal{G}}^{\mathrm{ev}}(\mathcal{T}_2) \tag{45}$$

that inserts a tensor factor of 1 in the slots of the new tetrahedra.

Lemma 4.4. $\phi_{2,0}$ is well-defined.

Proof. The description above certainly defines a map between the quantum tori. All Lagrangians and most edges of $\mathcal{T}_0$ are identical to those of $\mathcal{T}_2$. The only nontrivial check is the edge $\hat{E}$ shared by the two faces on the $\mathcal{T}_0$ side, which is split into two edges $\hat{E}', \hat{E}''$ on the $\mathcal{T}_2$ side. By inspection, we get $\phi_{2,0}(\hat{E}) = \hat{E}'\hat{E}''\hat{E}_0^{-1}$, where $\hat{E}_0 = \hat{Z}\hat{W}$ is the new vertical edge in Figure 7. Thus, $\phi_{3,2}(\langle \hat{E} - q \rangle_R)$ is still in $\langle \hat{E}_i - q \rangle_R$. □

Proposition 4.5. Suppose M has no non-peripheral $\mathbb{Z}/2$-homology. Then the quantum trace map is compatible with $\phi_{2,0}$ on the even part: $\widehat{\mathrm{tr}}_{\mathcal{T}_2} = \phi_{2,0} \circ \widehat{\mathrm{tr}}_{\mathcal{T}_0}$.

Proof. Let $\Sigma_i = \Sigma_{\mathcal{T}_i}$ be the dual surfaces. To go from Σ_0 to Σ_2, we remove a small neighborhood of the two A-circles in the move region and glue in the surface in Figure 8. Note two of the standard arcs in each removed annuli become standard arcs in the inserted surface, which are the horizontal ones in Figure 8.
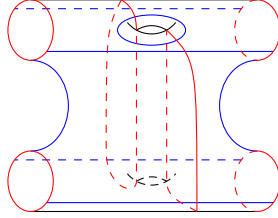
FIGURE 8. Surface inserted into Σ_0

In the calculation of $\widehat{\mathrm{tr}}_{\mathcal{T}_0}$, we can double the A-circles to make the annuli in the move region. We can also isotope any diagram to be standard arcs in the annuli that remain standard after the move. This gives 4 types of standard arcs (2 in each annuli). They evaluate to 0 or 1 by the counit depending on the states.

On the other hand, for $\widehat{\mathrm{tr}}_{\mathcal{T}_2}$, these standard arcs evaluate to 0 or $(\hat{Z}'\hat{W}'')^{\pm 1} = (\hat{Z}''\hat{W}')^{\mp 1}$. Again, $\hat{E}_0 = \hat{Z}\hat{W}$ is set to q in this statement. Now we reduce such a monomial using Lagrangians $L_z = \hat{Z}^{-1} + \hat{Z}'' - 1$ and $L_w'' = \hat{W}''^{-1} + \hat{W}' - 1$.

$$\begin{aligned}
\hat{Z}''\hat{W}' &= (1 - \hat{Z}^{-1} + L_z)\hat{W}' = (1 - \hat{E}_0^{-1}\hat{W})\hat{W}' + \hat{W}'L_z \\
&= \hat{W}' + q\hat{E}_0^{-1}\hat{W}''^{-1} + \hat{W}'L_z \\
&= 1 + L_w'' + \hat{W}'L_z + (q\hat{E}_0^{-1} - 1)\hat{W}''^{-1}.
\end{aligned} \tag{46}$$

Although $q\hat{E}_0^{-1} - 1$ does not commute with every term, it commutes with the whole $\hat{Z}''\hat{W}'$. Therefore, $(\hat{Z}''\hat{W}')^n - 1 \in \langle \hat{E}_0 - q \rangle_R + {}_L\langle L_z, L_w'' \rangle$ for $n \geq 0$. The same is true for $n < 0$ using an analogous calculation with $\hat{Z}'\hat{W}''$. This matches $\phi_{2,0} \circ \widehat{\mathrm{tr}}_{\mathcal{T}_0}$. $\qquad\square$

5. The 3d-index

In this section we review the 3d-index of [DGG13] and its relation to the normal surfaces of an ideal triangulation [GHHR16], following the notation of i.b.i.d. what is ibid?

As usual, we let $\mathbb{Z}[\![q^{1/2}]\!]$ (resp., $\mathbb{Z}(\!(q^{1/2})\!)$) denote the rings of formal power series (resp., formal Laurent series) in a variable $q^{1/2}$ with integer coefficients. Note $\mathbb{Z}(\!(q^{1/2})\!)$ is naturally a $\mathbb{Z}[q^{\pm 1/2}]$-module.

5.1. Tetrahedron index.
The DGG 3d-index is a sum over a lattice of products of building blocks, one per tetrahedron. The building block is the *tetrahedron index* $I_\Delta(m, e) \in \mathbb{Z}(\!(q^{1/2})\!)$ of [DGG13] defined by

$$I_\Delta(m, e) = \sum_{n=e_-}^{\infty} (-1)^n \frac{q^{\frac{1}{2}n(n+1) - (n+\frac{1}{2}e)m}}{(q;q)_n (q;q)_{n+e}}, \tag{47}$$

where $e_- = \max\{-e, 0\}$ and $(q;q)_n = \prod_{i=1}^{n}(1 - q^i)$ is the quantum factorial (also known as q-Pochhammer symbol).

The tetrahedron index satisfies some symmetries that can be conveniently expressed by saying that the 3-variable function

$$J_\Delta(a, b, c) = (-q^{1/2})^{-b} I_\Delta(b - c, a - b) \in \mathbb{Z}(\!(q^{1/2})\!) \tag{48}$$

is invariant under all six permutations of a, b, c, as was found out in [GHRS15, Sec.4.7]. These symmetries are reminiscent of the orbit of a shape of tetrahedron under all permutations (orientation preserving, or not).

In addition, the tetrahedron index satisfies a translation invariance, a linear q-difference equation, a pentagon identity and a quadratic identity:

$$J_\Delta(a - s, b - s, c - s) = (-q^{1/2})^s J_\Delta(a, b, c), \tag{49a}$$

$$q^{\frac{1}{2}(a-b)} J_\Delta(a, b, c - 1) + q^{\frac{1}{2}(c-b)} J_\Delta(a + 1, b, c) = J_\Delta(a, b, c), \tag{49b}$$

$$\sum_{k\in\mathbb{Z}} q^k J_\Delta(k, a + f, b + d) J_\Delta(k, a + e, c + d) J_\Delta(k, b + e, c + f) = J_\Delta(a, b, c) J_\Delta(d, e, f), \tag{49c}$$

$$\sum_{k\in\mathbb{Z}} q^k J_\Delta(a + k, c, d) J_\Delta(b + k, c, d) = q^{-a} \delta_{a,b}. \tag{49d}$$

Remark 5.1. It is easy to see that the tetrahedron index (47) is a series convergent on the unit disk $|q| < 1$. But more is true. Replacing q by q^{-1} in the q-hypergeometric sum, it follows that the tetrahedron index satisfies a duality

$$I_\Delta(m, e)(q^{-1}) = I_\Delta(-m, -e)(q), \qquad \text{or} \quad J_\Delta(a, b, c)(q^{-1}) = J_\Delta(-a, -b, -c)(q). \tag{50}$$

It follows that the tetrahedron index I_Δ as well as the symmetric form J_Δ are q-hypergeometric series that are convergent for $|q| \neq 1$.

Define the involution ι on the algebra of holomorphic functions of $q^{1/2} \in \mathbb{C}^\times \setminus S^1$ by

$$\iota(q^{1/2}) = q^{-1/2}. \tag{51}$$

Then we can write $\iota J_\Delta(a, b, c) = J_\Delta(-a, -b, -c)$.

5.2. **Basics on normal surfaces.** As we will see in the later section, there is a close connection between the 3d-index in the next section and normal surface theory. In this section we recall some basics on normal surface theory following the definitions from Sections 6–8 of [GHHR16] where the reader can find the references for the results stated below.

Normal surfaces were introduced by Haken and Kneser as a convenient way to deduce decision problems in 3-dimensional topology to piece-wise linear statements. Throughout this section, we fix a connected, oriented 3-manifold whose boundary consists of $r \geq 1$ torii, and an ideal triangulation $\mathcal{T}$ of M with N tetrahedra. A normal surface is S in M is a surface that intersects each tetrahedron in triangles or quadrilaterals. The number of triangles (there are four per tetrahedron) and quadrilaterals (three per tetrahedron) defines a vector in $\mathbb{N}^{7N} \subset \mathbb{R}^{7N}$ that satisfies some linear matching equations (one per face of $\mathcal{T}$), where $\mathbb{N} = \{0, 1, 2, \ldots\}$ is the set of nonnegative integers. Casson, Rubinstein and Tollefson noticed that normal surfaces can be uniquely reconstructed (up to multiples of peripheral surfaces) by their quadrilateral coordinates, and below we will be using only the quadrilateral coordinates

$$S = (a_1, b_1, c_1, \ldots, a_N, b_N, c_N) \in \mathbb{R}^{3N} \tag{52}$$

of a normal surface S. These coordinates satisfy a system of linear Q-matching equations, one per edge of $\mathcal{T}$. Since there are N edges, the $N \times 3N$ matrix of the Q-matching equations is given by $(A|B|C)D$ where $(A|B|C)$ is the $N \times 3N$ matrix of gluing equations of $\mathcal{T}$ with rows indexed by the edges of $\mathcal{T}$, and D is the block $3N \times 3N$ diagonal matrix of N copies of

$$\begin{pmatrix} 0 & 1 & -1 \\ -1 & 0 & 1 \\ 1 & -1 & 0 \end{pmatrix} \tag{53}$$

The vector space $\mathbb{R}^{3N}$ has a skew-symmetric pairing ω on $\mathbb{R}^{3N}$ defined as follows

$$\omega : \mathbb{R}^{3N} \times \mathbb{R}^{3N} \to \mathbb{R}, \qquad \omega(x, x') = x^t D x' = \sum_{j=1}^{N} \left(\begin{vmatrix} a_j & a'_j \\ b_j & b'_j \end{vmatrix} + \begin{vmatrix} b_j & b'_j \\ c_j & c'_j \end{vmatrix} + \begin{vmatrix} c_j & c'_j \\ a_j & a'_j \end{vmatrix} \right) \tag{54}$$

for

$$x = (a_1, b_1, c_1, \ldots, a_N, b_N, c_N), x' = (a'_1, b'_1, c'_1, \ldots, a'_N, b'_N, c'_N) \in (\mathbb{R}^3)^N. \tag{55}$$

The Q-matching equations can be expressed in terms of the skew-symmetric pairing as follows. $S \in \mathbb{R}^{3N}$ satisfies the Q-matching equations if and only if

$$\omega(E_i, S) = 0, \qquad i = 1, \ldots, n \tag{56}$$

where E_i is the ith row of $(A|B|C)$.

We denote by $Q(\mathcal{T}; \mathbb{R})$ the real Q-normal surface solution space. It is a real vector space that contains a lattice $Q(\mathcal{T}; \mathbb{Z})$ that consists of all $\mathbb{Z}$-solutions to the matching equations. There are three types of vectors in $Q(\mathcal{T}; \mathbb{Z})$, namely

- edge solutions E_i, for $i = 1, \ldots, N$ whose coordinates are the number of tetrahedra around the edge E_i for each quad type. This vector is exactly the exponent vector of the gluing (also known as Neumann–Zagier) equations of $\mathcal{T}$.
- tetrahedra solutions Δ_j for $j = 1, \ldots, N$ whose coordinates consist of $1, 1, 1$ in the j-th spots and 0 in all other spots.
- peripheral solutions M_k and L_k for $k = 1, \ldots, r$ whose coordinates are the exponent vectors of the cusp gluing equations of $\mathcal{T}$, with a fixed basis for the integer homology of each boundary torus.

While it is clear that the tetrahedra solutions satisfy the matching equations, the fact that the edge and the peripheral solutions satisfy the matching equations is equivalent to the symplectic property of the gluing equations proven by Neumann–Zagier, which asserts that all symplectic products of E_i, M_k, L_k for $i = 1, \ldots, N$ and $k = 1, \ldots, r$ are zero except that $\omega(L_k, M_k) = 2 = -\omega(M_k, L_k)$. Not all of the edge solutions are independent in $Q(\mathcal{T}; \mathbb{Z})$, but one can always find a suitable subset of $N - r$ independent edge solutions.

Kang–Rubinstein proved that the lattice $Q(\mathcal{T}; \mathbb{Z})$ has rank $2N + r$, with a basis that consists of $N - r$ edge solutions, N tetrahedra solutions and $2r$ peripheral solutions. On this lattice and its corresponding real vector space there is a linear function (an analogue of the Euler characteristic of a surface)

$$\chi : Q(\mathcal{T}; \mathbb{R}) \to \mathbb{R}, \qquad \chi(S) = \sum_i -2x_i - \sum_j y_j \tag{57}$$

defined for

$$S = \sum_i x_i E_i + \sum_j y_j \Delta_j + \sum_k (p_k M_k + q_k L_k). \tag{58}$$

The vector space $\mathbb{R}^{3N}$ has a quadratic form, the double-arc function, defined as follows

$$\delta : \mathbb{R}^{3N} \to \mathbb{R}, \qquad \delta(x) = \frac{1}{2} x^t D^{\mathrm{sym}} x = \sum_{j=1}^N (a_j b_j + b_j c_j + c_j a_j) \tag{59}$$

where D^{sym} is the block $3N \times 3N$ diagonal matrix of N copies of

$$\begin{pmatrix} 0 & 1 & 1 \\ 1 & 0 & 1 \\ 1 & 1 & 0 \end{pmatrix} \tag{60}$$

and x is as in (55). Its corresponding bilinear form is given by

$$\delta : \mathbb{R}^{3N} \times \mathbb{R}^{3N} \to \mathbb{R}, \qquad \delta(x, x') = \frac{1}{2} x^t D^{\mathrm{sym}} x'. \tag{61}$$

The double-arc function determines the $q^{1/2}$-degree of the tetrahedron index in its symmetric version $J_\Delta(a, b, c)$; see [GHHR16, Eqn.(8)]

$$\deg J_\Delta(a, b, c) = \delta(a - m, b - m, c - m) - m, \qquad m = \min\{a, b, c\}. \tag{62}$$

δ satisfies a positivity property: for all $x, x' \in \mathbb{R}_+^{3N}$ (where $\mathbb{R}_+ = [0, \infty)$) we have

$$\delta(x + x') \geq \delta(x) + \delta(x'), \tag{63}$$

which is a consequence of the fact that D has nonnegative entries.

The lattice $Q(\mathcal{T}; \mathbb{Z})$ contains a sublattice $Q_0(\mathcal{T}; \mathbb{Z})$ of solutions of Q-matching equations corresponding to closed surfaces of rank $2N - r$ with basis $N - r$ edge solutions generating a sublattice $\mathbb{E}$ and N tetrahedra solutions generating a sublattice $\mathbb{\Delta}$. It is this lattice that will play a role in the 3d-index through the bijection

$$\mathbb{Z}^{N-r} \simeq Q_0(\mathcal{T}; \mathbb{Z})/\mathbb{\Delta} = (\mathbb{E} + \mathbb{\Delta})/\mathbb{\Delta}, \qquad k = (k_1, \ldots, k_{N-r}) \mapsto S(k) = \sum_{i=1}^{N-r} k_i E_i. \qquad (64)$$

5.3. **Definition of the 3d-index.** We now have all the ingredients to define the 3d-index. We fix an 1-efficient triangulation $\mathcal{T}$ with N tetrahedra on an oriented 3-manifold with r torus boundary components.

Let $\mathbb{T}_{\mathcal{T}}^{\mathrm{ev}} := \bigotimes_{j=1}^{N} \mathbb{T}^{\mathrm{ev}} \langle \hat{Z}_j, \hat{Z}'_j, \hat{Z}''_j \rangle$. It has the Weyl-ordered basis $\{[\vec{Z}^S] \mid S \in \mathbb{Z}^{3N}\}$ where

$$\vec{Z}^S = \prod_{j=1}^{N} \hat{Z}_j^{a_j} (\hat{Z}'_j)^{b_j} (\hat{Z}''_j)^{c_j}, \qquad S = (a_1, b_1, c_1, \ldots, a_N, b_N, c_N) \in \mathbb{Z}^{3N} \qquad (65)$$

Note $[\vec{Z}^{E_i}] = \hat{E}_i$, and $[\vec{Z}^{\Delta_j}] = [\hat{Z}_j \hat{Z}'_j \hat{Z}''_j]$. Note also that the q-commuting relations (30) (after squaring) matches the definition (54).

Definition 5.2. Consider the unique $\mathbb{Z}[q^{\pm 1/2}]$-linear map

$$I_{\mathcal{T}} : \mathbb{T}_{\mathcal{T}}^{\mathrm{ev}} = \bigotimes_{j=1}^{N} \mathbb{T}^{\mathrm{ev}} \langle \hat{Z}_j, \hat{Z}'_j, \hat{Z}''_j \rangle \to \mathbb{Z}(\!(q^{1/2})\!) \qquad (66)$$

given by the following series in $\mathbb{Z}(\!(q^{1/2})\!)$

$$I_{\mathcal{T}}([\vec{Z}^{S_0}]) = \sum_{k \in \mathbb{Z}^{N-r}} (-q^{\frac{1}{2}})^{-\chi(S(k))} q^{\frac{1}{2}\omega(S_0, S(k))} J\left(-S_0 + S(k)\right), \qquad (67)$$

where J is the extension of J_Δ from $\mathbb{Z}^3$ to $\mathbb{Z}^{3N}$ by

$$J : \mathbb{Z}^{3N} \to \mathbb{Z}(\!(q^{1/2})\!), \qquad S = (a_1, b_1, c_1, \ldots, a_N, b_N, c_N) \mapsto \prod_{j=1}^{N} J_\Delta(a_j, b_j, c_j). \qquad (68)$$

Theorem 5.3. $I_{\mathcal{T}}$ is well-defined (i.e., its image are convergent power series in $\mathbb{Z}(\!(q^{1/2})\!)$).
  If M has no non-peripheral $\mathbb{Z}/2$-homology, then $I_{\mathcal{T}}$ descends to a map

$$I_{\mathcal{T}} : \widehat{\mathcal{G}}^{\mathrm{ev}}(\mathcal{T}) \to \mathbb{Z}(\!(q^{1/2})\!). \qquad (69)$$

Proof. Using the bijection (64), we can rewrite the definition as

$$I_{\mathcal{T}}([\vec{Z}^{S_0}]) = \sum_{[S] \in Q_0(\mathcal{T}; \mathbb{Z})/\mathbb{\Delta}} (-q^{\frac{1}{2}})^{-\chi(S)} q^{\frac{1}{2}\omega(S_0, S)} J(-S_0 + S). \qquad (70)$$

Note the summand does not depend on the representative S, since $(-q^{\frac{1}{2}})^{-\chi(S)} J(-S_0 + S)$ is well-defined by [GHHR16, Section 8], and $\omega(*, \Delta_j) = 0$ by direct calculation.

First, we prove the convergence of our extended 3d-index for $S_0 \in \mathbb{Z}^{3N}$. The case $S_0 \in Q_0(\mathcal{T}; \mathbb{Z})$ is covered by [GHHR16, Theorem 8.6], so we assume $S_0 \notin Q_0(\mathcal{T}; \mathbb{Z})$. In this case, we follow the proof of [GHHR16, Theorem 8.8].

Let

$$Q_{S_0}(\mathcal{T};\mathbb{Z}) = \mathbb{Z}S_0 \oplus Q_0(\mathcal{T};\mathbb{Z}), \qquad Q^1_{S_0}(\mathcal{T};\mathbb{Z}) = (-S_0) + Q_0(\mathcal{T};\mathbb{Z}) \subset Q_{S_0}(\mathcal{T};\mathbb{Z}). \tag{71}$$

Define $\chi_{S_0}(kS_0 + S') = \chi(S')$ for any $k \in \mathbb{Z}$ and $S' \in Q_0(\mathcal{T};\mathbb{Z})$. Then the definition (70) can be rewritten once again as

$$I_{\mathcal{T}}([\vec{Z}^{S_0}]) = \sum_{[S] \in Q^1_{S_0}(\mathcal{T};\mathbb{Z})/\triangle} (-q^{\frac{1}{2}})^{-\chi_{S_0}(S)} q^{\frac{1}{2}\omega(S_0,S)} J(S). \tag{72}$$

We can choose $\triangle$-coset representatives which are convenient for the degree formula (62). Given $S \in \mathbb{Z}^{3N}$, there is a unique translation S^* by an element of $\triangle$ such that $\min\{a_j, b_j, c_j\} = 0$ for every $j = 1, \ldots, N$. (If $S \in Q(\mathcal{T};\mathbb{Z})$, then the corresponding normal surface has at most two types of quads at each tetrahedron). This defines an injective map $\mathbb{Z}^{3N}/\triangle \to \mathbb{N}^{3N}$. Then the sum in (72) can be replaced by $S^* \in Q^{1*}_{S_0}(\mathcal{T};\mathbb{N}) := (Q^1_{S_0}(\mathcal{T};\mathbb{Z})/\triangle)^*$, and the degree of the summand is

$$d(S^*) = -\chi_{S_0}(S^*) + \omega(S_0, S^*) + \delta(S^*). \tag{73}$$

Let $Q^*_{S_0}(\mathcal{T};\mathbb{N}) = \big(\mathbb{N}(-S_0) + Q^*_0(\mathcal{T};\mathbb{Z})\big) \cap \mathbb{N}^{3N}$. This is the intersection of a lattice with a rational polyhedral cone, hence every vector in $Q^*_{S_0}(\mathcal{T};\mathbb{N})$ is an $\mathbb{N}$-linear combination of a finite set F_i of fundamental solutions. Let I_0 and I_1 denote the set of i that correspond to fundamental solutions F_i in $Q_0(\mathcal{T};\mathbb{N})$ and $Q^{1*}_{S_0}(\mathcal{T};\mathbb{N})$ respectively. Then for $S^* \in Q^{1*}_{S_0}(\mathcal{T};\mathbb{N})$, we can write

$$S^* = F_k + \sum_{i \in I_0} x_i F_i \qquad \text{for some } k \in I_1 \text{ and } x_i \in \mathbb{N}. \tag{74}$$

The function d is defined for all of $Q^*_{S_0}(\mathcal{T};\mathbb{N})$. By (63) and the linearity of the first two terms, d is superadditive, so for S^* as above,

$$d(S^*) \geq d(F_k) + \sum_{i \in I_0} d(x_i F_i). \tag{75}$$

For $i \in I_0$, consider the term

$$d(x_i F_i) = -\chi(F_i)x_i + \delta(F_i)x_i^2, \qquad x_i \geq 0. \tag{76}$$

Since $\mathcal{T}$ is 1-efficient, for each i, we have either $\delta(F_i) = 0$ and $-\chi(F_i) \geq 1$ or $\delta(F_i) \geq 1$. Therefore, $d(x_i F_i) \to \infty$ as $x_i \to \infty$. Since there are finitely many choices of $F_k, k \in I_1$, and $d(S^*) \to \infty$ if any $x_i \to \infty$, we see $d(S^*) \leq D$ has finitely many solutions S^*. This implies the convergence of (72).

Now we show that $I_{\mathcal{T}}$ is compatible with the quotient $\mathbb{T}^{\mathrm{ev}}_{\mathcal{T}} \twoheadrightarrow \widehat{\mathcal{G}}^{\mathrm{ev}}(\mathcal{T})$. By the homology condition, $\widehat{\mathcal{G}}^{\mathrm{ev}}(\mathcal{T})$ is given by the presentation (35) (with $\hat{Z}'_j$ restored). This means we need to check

(a) $I_{\mathcal{T}}(\hat{E}_i[\vec{Z}^{S_0}]) = qI_{\mathcal{T}}([\vec{Z}^{S_0}])$.
(b) $I_{\mathcal{T}}([\hat{Z}_j \hat{Z}'_j \hat{Z}''_j][\vec{Z}^{S_0}]) = -q^{\frac{1}{2}}I_{\mathcal{T}}([\vec{Z}^{S_0}])$.
(c) $I_{\mathcal{T}}([\vec{Z}^{S_0}](\hat{Z}_j^{-1} + \hat{Z}''_j - 1)) = 0$.

For (a), as remarked after the definition (31) of $\widehat{\mathcal{G}}(\mathcal{T})$, we only need to consider $i = 1, \ldots, N - r$. Since $\hat{E}_i[\vec{Z}^{S_0}] = q^{\frac{1}{2}\omega(E_i, S_0)}[\vec{Z}^{S_0 + E_i}]$, it follows that

$$
\begin{aligned}
I_{\mathcal{T}}(\hat{E}_i[\vec{Z}^{S_0}]) &= q^{\frac{1}{2}\omega(E_i, S_0)} I_{\mathcal{T}}([\vec{Z}^{S_0 + E_i}]) \\
&= q^{\frac{1}{2}\omega(E_i, S_0)} \sum_{[S] \in Q_0(\mathcal{T};\mathbb{Z})/\mathbb{A}} (-q^{\frac{1}{2}})^{-\chi(S)} q^{\frac{1}{2}\omega(S_0 + E_i, S)} J(-S_0 - E_i + S) .
\end{aligned} \tag{77}
$$

Since $E_i \in Q_0(\mathcal{T}; \mathbb{Z})$, shifting $S \mapsto S + E_i$, we obtain that

$$
I_{\mathcal{T}}(\hat{E}_i[\vec{Z}^{S_0}]) = q^{\frac{1}{2}\omega(E_i, S_0)} \sum_{[S] \in Q_0(\mathcal{T};\mathbb{Z})/\mathbb{A}} (-q^{\frac{1}{2}})^{-\chi(S + E_i)} q^{\frac{1}{2}\omega(S_0 + E_i, S + E_i)} J(-S_0 + S). \tag{78}
$$

Definition (57) implies that $\chi(E_i) = -2$ and (56) implies that $\omega(E_i, S) = 0$. This gives that $\omega(S_0 + E_i, S + E_i) = \omega(S_0, S) + \omega(S_0, E_i)$. Together with the above, we get

$$
I_{\mathcal{T}}(\hat{E}_i[\vec{Z}^{S_0}]) = q I_{\mathcal{T}}([\vec{Z}^{S_0}]), \tag{79}
$$

which concludes part (a).

For part (b), since $\omega(\Delta_j, *) = 0$, we have

$$
\begin{aligned}
I_{\mathcal{T}}([\hat{Z}_j \hat{Z}_j' \hat{Z}_j''][\vec{Z}^{S_0}]) &= I_{\mathcal{T}}([\vec{Z}^{S_0 + \Delta_i}]) \\
&= \sum_{[S] \in Q_0(\mathcal{T};\mathbb{Z})/\mathbb{A}} (-q^{\frac{1}{2}})^{-\chi(S)} q^{\frac{1}{2}\omega(S_0, S)} J(-S_0 - \Delta_i + S) .
\end{aligned} \tag{80}
$$

By (49a), the $-\Delta_i$ can be replaced by a factor of $-q^{\frac{1}{2}}$, which proves part (b). Finally, part (c) follows similarly from the linear q-difference equation (49b) for the tetrahedron index.

This completes the proof of the theorem. $\qquad\square$

Remark 5.4. Still assume that M has no non-peripheral $\mathbb{Z}/2$-homology. There is a bijection of $Q_0(\mathcal{T};\mathbb{Z})/\mathbb{A}$ with the set of embedded generalized normal surfaces (see [GHHR16, Eqn.(35)]) which converts the sum (70) as a generating function over the set of embedded generalized normal surfaces (i.e., embedded surfaces that intersect each tetrahedron in a polygon with a number of sides divisible by 4).

5.4. **Compatibility with 3–2 and 2–0 moves.** In this section we study how the map (69) changes under moves on the triangulation. By the same proof as parts (b) and (c) of the invariance in Theorem 5.3, the map

$$
I_N : \bigotimes_{j=1}^{N} \mathbb{T}^{\mathrm{ev}}\langle \hat{Z}_j, \hat{Z}_j', \hat{Z}_j'' \rangle \to \mathbb{Z}((q^{1/2})), \qquad I_N([\vec{Z}^S]) = J(-S) \tag{81}
$$

descends to $\bigotimes_{j=1}^{N} \widehat{\mathcal{G}}^{\mathrm{ev}}(\mathbb{L}_j) \to \mathbb{Z}((q^{1/2}))$. Note the homology condition is only used to show that there are no extra relations from edges, so the tetrahedron solutions and Lagrangians are not affected.

Given $S = S(k) \in \mathbb{E}$, note

$$
\mathcal{E}_S := (-q^{\frac{1}{2}})^{-\chi(S)} [\vec{Z}^{-S}] = \prod_{i=1}^{N-r} (q \hat{E}_i^{-1})^{k_i}, \tag{82}
$$

and $q^{\frac{1}{2}\omega(S_0,S)}$ is the Weyl-ordering factor for $\left[[\vec{Z}^{-S}][\vec{Z}^{S_0}]\right]$. Then we have yet another formula for the index

$$I_{\mathcal{T}}(x) = \sum_{S \in \mathbb{E}} I_N(\mathcal{E}_S \cdot x). \tag{83}$$

Proposition 5.5. Suppose M has no non-peripheral $\mathbb{Z}/2$-homology. The triangulation index is compatible with the maps (41) and (45)

$$I_{\mathcal{T}_2} = I_{\mathcal{T}_3} \circ \phi_{3,2}, \qquad I_{\mathcal{T}_0} = I_{\mathcal{T}_2} \circ \phi_{2,0}. \tag{84}$$

Proof. This is a straightforward generalization of Theorem 4.3 and A.1 in [GHRS15], so we omit some details.

First consider the 3–2 move. We use the notations of Section 4.1. As in [GHRS15, Theorem A.1], we can choose the independent edges of $\mathcal{T}_2$ such that adding the new edge E_0 of $\mathcal{T}_3$ gives an independent set of edges in $\mathcal{T}_3$. Thus,

$$I_{\mathcal{T}_3}(\phi_{3,2}(x)) = \sum_{S \in \mathbb{E}_2} \sum_{k \in \mathbb{Z}} I_{N+1}\left((q\hat{E}_0^{-1})^k \cdot \phi_{3,2}(\mathcal{E}_S \cdot x)\right). \tag{85}$$

Let x be a monomial and write $\mathcal{E}_S \cdot x = [\hat{Z}^a \hat{Z}'^b \hat{Z}''^c][\hat{W}^d \hat{W}'^e \hat{W}''^f]\tilde{x} \in \widehat{\mathcal{G}}^{\mathrm{ev}}(\mathcal{T}_2)$. By definition, $\phi_{3,2}(\mathcal{E}_S \cdot x)$ is the monomial $[\hat{X}'^{a+f}\hat{X}''^{b+d}][\hat{Y}'^{b+e}\hat{Y}''^{c+f}][\hat{V}'^{c+d}\hat{V}''^{a+e}]\tilde{x}$. Then the sum over k can be evaluated using the pentagon identity (49c), recalling that $\hat{E}_0 = \hat{X}\hat{Y}\hat{V}$. The remaining sum is exactly $I_{\mathcal{T}_2}(x)$.

The 2–0 move is similar. We use the notations of Section 4.2. Recall the shared edge in the move region of $\mathcal{T}_0$ is denoted E, which splits into two edges E', E'' in $\mathcal{T}_2$, and the additional central edge in $\mathcal{T}_2$ is denoted E_0.

Using [GHRS15, Theorem 4.3], we can choose E to be part of the independent edges of $\mathcal{T}_0$, and a set of independent edges for $\mathcal{T}_2$ can be obtained by replacing E with E_0, E', E''. Write

$$\mathbb{E}_0 = \mathbb{Z}E \oplus \tilde{\mathbb{E}}_0, \qquad \mathbb{E}_2 = \mathbb{Z}E_0 \oplus \mathbb{Z}E' \oplus \mathbb{Z}E'' \oplus \tilde{\mathbb{E}}_0. \tag{86}$$

Then

$$I_{\mathcal{T}_0}(x) = \sum_{S \in \tilde{\mathbb{E}}_0} \sum_{a \in \mathbb{Z}} I_N\left((q\hat{E}^{-1})^a \cdot \mathcal{E}_S \cdot x\right), \tag{87}$$

$$I_{\mathcal{T}_2}(\phi_{2,0}(x)) = \sum_{S \in \tilde{\mathbb{E}}_0} \sum_{(a,b) \in \mathbb{Z}^2} \sum_{k \in \mathbb{Z}} I_{N+2}\left((q\hat{E}_0^{-1})^k (q\hat{E}'^{-1})^a (q\hat{E}''^{-1})^b \cdot \phi_{2,0}(\mathcal{E}_S \cdot x)\right). \tag{88}$$

In $I_{\mathcal{T}_2}(\phi_{2,0}(x))$, the sum over k can be evaluated using (49d), resulting in $q^{-a}\delta_{a,b}$, deleting $\hat{Z}$ and $\hat{W}$ from $\hat{E}'$ and $\hat{E}''$, and combining them into $(q\hat{E}^{-1})^a$. This agrees with $I_{\mathcal{T}_0}(x)$. $\square$

Combining this with Propositions 4.2 and 4.5, we get the commutative diagrams of Equation (5).

Remark 5.6. Now that all the pieces are defined, we sketch the generalization of the 3d-index to manifolds with non-peripheral $\mathbb{Z}/2$-homology.

In this case, by [GHHR16, Theorem 7.1], $Q_0(\mathcal{T};\mathbb{Z})$ is only a subgroup of the lattice of normal surfaces $N(\mathcal{T};\mathbb{Z})$, and the quotient is isomorphic to the cokernel of $H_1(\partial M;\mathbb{Z}/2) \to H_1(M;\mathbb{Z}/2)$, which is finite and independent of the triangulation $\mathcal{T}$.

The first instances of the homology restriction are Lemma 3.3 and Proposition 3.4. The lattice Λ there is isomorphic to $Q_0(\mathcal{T}; \mathbb{Z})/\mathbb{A}$, and we can show that $\Lambda^\perp$ is isomorphic to $N(\mathcal{T}; \mathbb{Z})/\mathbb{A}$, and $\Lambda^\perp = (\frac{1}{2}\Lambda) \cap \mathbb{Z}^{2N}$. The even edge relation $\hat{E}_i - q = [\vec{Z}^{E_i}] - (-q^{1/2})^{-\chi(E_i)}$ should be generalized to $[\vec{Z}^S] - (-q^{1/2})^{-\chi(S)}$ for all $S \in N(\mathcal{T}; \mathbb{Z})/\mathbb{A}$ when there is non-peripheral $\mathbb{Z}/2$-homology.

Proposition 4.5 also has the homology restriction, but it follows from the presentation in Proposition 3.4. As mentioned in Remark 4.3, 2–0 move can be modified to work in the full $\widehat{\mathcal{G}}(\mathcal{T})$, so the homology restriction is naturally dropped in this case.

Instead of summing over $Q_0(\mathcal{T}; \mathbb{Z})/\mathbb{A}$ in (70), the generalization of the index should sum over $N(\mathcal{T}; \mathbb{Z})/\mathbb{A}$. By partitioning into cosets of $N(\mathcal{T}; \mathbb{Z})/Q_0(\mathcal{T}; \mathbb{Z})$, we see that the generalization is an extra finite sum, so the convergence and compatibility with moves are unaffected. Since the presentation of $\widehat{\mathcal{G}}^{\mathrm{ev}}(\mathcal{T})$ has the same modification, the descent to I_M also works.

5.5. **Insertion of peripheral elements.** Recall the vectors $M_k, L_k \in \mathbb{Z}^{3N}$ defined in Section 5.2, which are associated to a basis μ_k, λ_k of $H_1(\partial M; \mathbb{Z})$. We get a vector C_γ for each $\gamma \in H_1(\partial M; \mathbb{Z})$ by making linear combinations. Define

$$\hat{m}_\gamma = [\vec{z}^{C_\gamma}] \in \bigotimes_{j=1}^N \mathbb{T}\langle \hat{z}_j, \hat{z}_j', \hat{z}_j'' \rangle. \tag{89}$$

By the symplectic relations among M_k, L_k, the monomials $\hat{m}_\gamma$ from different boundary components commute with each other. Therefore, we focus on a single component in the following.

If γ reduces to 0 in $H_1(M; \mathbb{Z}/2)$, then $\hat{m}_\gamma$ is in the even part. Then the DGG index with class γ is simply $I_\mathcal{T}(\hat{m}_\gamma)$. In terms of charges, we have Equation (3). If we choose λ to be the homological longitude. Then m can take half integer values.

Although $\hat{m}_\gamma$ is not technically in $\mathcal{S}(M)$, it can be included by an extension. This requires a quick review of the skein algebra of the torus T^2.

Model the torus as $T^2 = \mathbb{R}^2/\mathbb{Z}^2$ such that the curves in the directions $(1, 0)$ and $(0, 1)$ are the longitude λ and meridian μ. Given a nonzero $\gamma \in H_1(T^2; \mathbb{Z})$, we can write $\gamma = s\lambda + t\mu$. If s, t are coprime, define K_γ as the simple closed curve in the direction (s, t). More generally, if $\gcd(s, t) = d$, then $K_\gamma \in \mathcal{S}(T^2)$ is defined as $T_d(K_{s/d, t/d})$, where $T_n(x)$ is the Chebyshev polynomial given by

$$T_0(x) = 2, \qquad T_1(x) = x, \qquad T_n(x) = x T_{n-1}(x) - T_{n-2}(x), \quad n \geq 2. \tag{90}$$

These elements together with 1 form a basis of $\mathcal{S}(T^2)$. This is used in [FG00] to obtain an algebra embedding

$$\mathcal{S}(T^2) \hookrightarrow \mathbb{T}\langle \hat{m}_\lambda, \hat{m}_\mu \rangle, \qquad K_\gamma \mapsto \hat{m}_\gamma + \hat{m}_\gamma^{-1}. \tag{91}$$

Now back to the 3-manifold M. For each torus boundary component, a choice of the longitude λ and meridian μ defines a map $\mathcal{S}(T^2) \to \mathcal{S}(M)$. In fact, $\mathcal{S}(T^2)$ acts on $\mathcal{S}(M)$ since gluing $T^2 \times [-1, 1]$ to the torus boundary does not change the manifold. We choose to glue along $T^2 \times \{-1\}$ so that the action is on the left.

A related action is defined on the quantum gluing module. By the symplectic properties mentioned in Section 5.2, the peripheral monomials $\hat{m}_\gamma$ commutes with the edges $\hat{e}_i$. Thus, the quantum torus $\mathbb{T}\langle \hat{m}_\lambda, \hat{m}_\mu \rangle$ acts on $\widehat{\mathcal{G}}(\mathcal{T})$ from the left.

Theorem 5.7. *The actions above are related by the quantum trace and the embedding* (91). *In other words,*

$$\widehat{\mathrm{tr}}_{\mathcal{T}}(K_\gamma \cdot \alpha) = (\hat{m}_\gamma + \hat{m}_\gamma^{-1}) \cdot \widehat{\mathrm{tr}}_{\mathcal{T}}(\alpha). \tag{92}$$

The classical trace obviously has this property, so by the classical limit given in [GY, Theorem 1.1], the quantum trace is given by the same formula up to $q^{1/8} - q^{-1/8}$. The nontrivial part of the theorem is proving that all quantum corrections vanishes, which is not obvious since certain intermediate stages could have correction terms (see e.g. Lemma A.1). The proof is given in Appendix A.

The theorem implies that the composed index $I_M : \mathcal{S}^{\mathrm{ev}}(M) \to \mathbb{Z}((q^{1/2}))$ from (6) can be extended to

$$\mathbb{T}\langle \hat{m}_\mu^2, \hat{m}_\lambda \rangle \otimes_{\mathcal{S}'(T^2)} \mathcal{S}^{\mathrm{ev}}(M) \to \mathbb{Z}((q^{1/2})). \tag{93}$$

Here, $\mathcal{S}'(T^2)$ is the subalgebra of $\mathcal{S}(T^2)$ where the homology grading is even in μ but arbitrary in λ, which is chosen to be a homological longitude. This corresponds to the index $\mathcal{I}_{M+\hat{O}_K}(m, e)$ conjectured by [AGLR], where m, e defines the monomial in $\mathbb{T}\langle \hat{m}_\mu^2, \hat{m}_\lambda \rangle$ in the same way as the DGG index, and $K \in \mathcal{S}^{\mathrm{ev}}(M)$.

5.6. **Chirality.** In this section we discuss the behavior of our maps under the (involution) operation of reversing the orientation of the ambient 3-manifold. As always, M denotes a compact oriented 3-manifold with torus boundary and $\mathcal{T}$ an ideal triangulation of M. Denote by $-M$ the same manifold with the opposite orientation.

Starting with the skein module, we see the crossing in (7) is flipped when the orientation is reversed. Recalling the involution ι from (51), there is an ι-conjugate linear map $\mathcal{S}(M) \to \mathcal{S}(-M)$ sending a framed link to itself, denoted also by ι by abuse of notation. For the stated skein algebras and corner-reduced skein modules, to preserve the defining relations (8), (9), and (13), it is also necessary to flip the states. Then we also get an ι-conjugate algebra map $\iota : \mathcal{S}(\Sigma) \to \mathcal{S}(-\Sigma)$ and an ι-conjugate linear map $\iota : \mathcal{S}_{\mathrm{cr}}(\Sigma) \to \mathcal{S}_{\mathrm{cr}}(-\Sigma)$.

Now consider the quantum gluing modules. $-M$ has a triangulation $-\mathcal{T}$ obtained from $\mathcal{T}$ by relabeling the vertices to change the orientations of all tetrahedra. This can be done systematically by exchanging vertices 1 and 3 for all tetrahedra, which has the effect $\hat{z} \leftrightarrow \hat{z}''$. Considering the state flipping in skein modules, the correct correspondence is

$$\iota(\hat{z}) = \hat{z}''^{-1}, \quad \iota(\hat{z}'') = \hat{z}^{-1}. \tag{94}$$

The inverse is also necessary for the Lagrangian equation. Putting it all together, we get an ι-conjugate map $\iota : \widehat{\mathcal{G}}(\mathcal{T}) \to \widehat{\mathcal{G}}(-\mathcal{T})$.

These maps can be combined into the following commutative diagram.

$$\begin{array}{ccccc}
\mathcal{S}^{\mathrm{ev}}(M) & \xrightarrow{\widehat{\mathrm{tr}}_{\mathcal{T}}} & \widehat{\mathcal{G}}^{\mathrm{ev}}(\mathcal{T}) & \xrightarrow{I_{\mathcal{T}}} & \mathbb{Z}((q^{1/2})) \\
\downarrow{\iota} & & \downarrow{\iota} & & \downarrow{\iota} \\
\mathcal{S}^{\mathrm{ev}}(-M) & \xrightarrow{\widehat{\mathrm{tr}}_{-\mathcal{T}}} & \widehat{\mathcal{G}}^{\mathrm{ev}}(-\mathcal{T}) & \xrightarrow{I_{-\mathcal{T}}} & \mathbb{Z}((q^{1/2}))
\end{array} \tag{95}$$

The left square commutes by definition and the discussion above. The right square commutes by definition and the duality (50). This means $I_{-M} \circ \iota = \iota \circ I_M$.

[AGLR] conjectured a symmetry

$$I_M(\hat{m}_\gamma \otimes K) = I_M(\hat{m}_\gamma^{-1} \otimes K) \tag{96}$$

for the peripheral-extended 3d-index (93). We did not find any theoretical reason for this to hold in general. In the specific example of 4_1 that [AGLR] considered, it can be explained by the reversibility of 4_1. On a related note, the restriction to DGG index, that is, when $K = 1$, satisfies

$$I_M(\hat{m}_\gamma^{-1}) = \iota I_M(\hat{m}_\gamma) = I_M(\hat{m}_\gamma)(q^{-1}). \tag{97}$$

This is obtained by replacing $k \leftrightarrow -k$ in the sum in (67).

6. EXAMPLE: THE 4_1 KNOT

Let M be the complement of the 4_1 knot. The default triangulation $\mathcal{T}$ of M with isometry signature cPcbbbiht_BaCB has two tetrahedra T_0 and T_1 shown in Figure 9 using the convention from Figure 3. There are 4 face pairings labeled A,B,C,D.
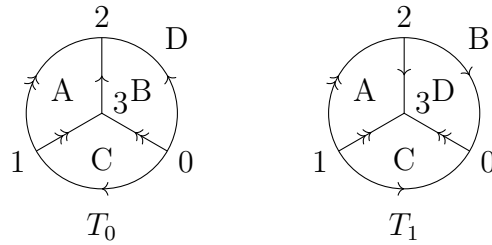

FIGURE 9. SnapPy triangulation of the 4_1 knot.

The dual surface $\Sigma_\mathcal{T}$ is obtained in [GY, Section 6.2] and reproduced in Figure 10, which is $\Sigma_\mathcal{T}$ split along the A-circles. The region labeled $i + 4j$ in black corresponds to the vertex i in T_j, and dually, the red A-circle labeled $i + 4j$ is the face opposite to vertex i in T_j. The small red labels around the A-circles indicate how the lanterns glue together to form $\Sigma_\mathcal{T}$. The arrow on a blue standard arc indicates which edge of $\mathcal{T}$ it goes around.
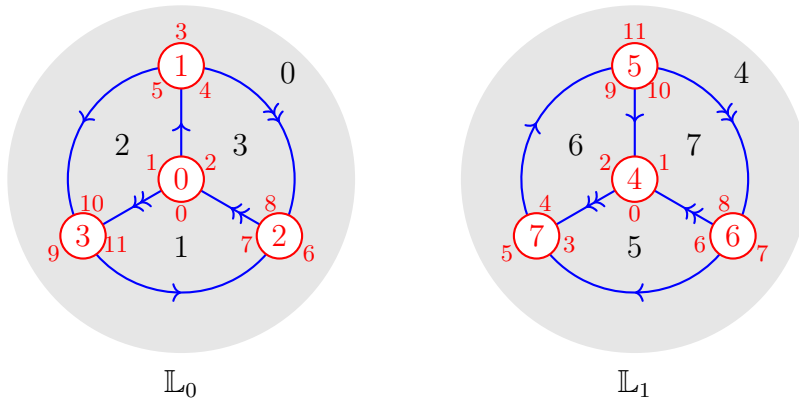

FIGURE 10. Lantern diagram for the 4_1 knot.

The quantum trace of the meridian μ was calculated in [GY, Section 6.2] in agreement with Theorem 5.7. Let K_b be the knot in M shown in Figure 11, and let $K_b^{(2)}$ be the 2-parallel. By [BLF05, Theorem 2.1], $\mu^n \cdot K_b$ and $\mu^n \cdot K_b^{(2)}$ is a basis of $\mathcal{S}(M)$. Thus, $\widehat{\mathrm{tr}}_{\mathcal{T}}(K_b)$ and $\widehat{\mathrm{tr}}_{\mathcal{T}}(K_b^{(2)})$ determine the entire quantum trace map by Theorem 5.7.
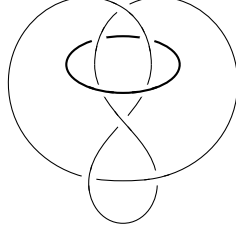

FIGURE 11. The knot K_b in the complement of 4_1.

The lantern diagram of K_b is given in Figure 12. To calculate its quantum trace, we assign matching states to the endpoints of the arcs. Because of the standard arc in $\mathbb{L}_0$, the only nonzero terms are the all $+$ and all $-$ states. Then by twisting the arc in $\mathbb{L}_1$ using Lemma 2.1, we get

$$\widehat{\mathrm{tr}}_{\mathcal{T}}(K_b) = q^{-1/2}(\hat{z}_0'^{-1}(\hat{z}_1'^{-1} - \hat{z}_1') - \hat{z}_0'\hat{z}_1'^{-1}) \in \widehat{\mathcal{G}}(\mathcal{T}). \tag{98}$$

Since K_b has 0 linking number with 4_1, it has 0 homology in M, and it is an element of the even skein module $\mathcal{S}^{\mathrm{ev}}(M)$. However, the diagram Figure 12 does not have 0 homology on $\Sigma_{\mathcal{T}}$, so the quantum trace (98) calculated from this diagram is not obviously in the even gluing module $\widehat{\mathcal{G}}^{\mathrm{ev}}(\mathcal{T})$. This can be fixed by using $\hat{e}_0 = [\hat{z}_0^2\hat{z}_0'\hat{z}_1^2\hat{z}_1']$ and $[\hat{z}_j\hat{z}_j'\hat{z}_j''] = \mathbf{i}q^{1/4}$ to rewrite $\widehat{\mathrm{tr}}_{\mathcal{T}}(K_b) = (-q^{1/2}\hat{e}_0^{-1})\widehat{\mathrm{tr}}_{\mathcal{T}}(K_b)$ as

$$\widehat{\mathrm{tr}}_{\mathcal{T}}(K_b) = -q^{-1/2}(\hat{Z}_0^{-1}\hat{Z}_1'' + \hat{Z}_0''\hat{Z}_1^{-1} + \hat{Z}_0''\hat{Z}_1'') \in \widehat{\mathcal{G}}^{\mathrm{ev}}(\mathcal{T}). \tag{99}$$

This agrees with the conjecture of [AGLR] and matches the calculations of [PP] up to conventions. The same calculation can be done with $K_b^{(2)}$, the result given by

$$\widehat{\mathrm{tr}}_{\mathcal{T}}(K_b^{(2)}) = q^{-2}\hat{Z}_0'^{-1}\hat{Z}_1'^{-1} + q^{-1}(\hat{Z}_0'\hat{Z}_1'^{-1} + \hat{Z}_0'^{-1}\hat{Z}_1') - (q^{-1}+q^{-2})(\hat{Z}_0'^{-1}+\hat{Z}_1'^{-1}) + q^{-2} + 1. \tag{100}$$

This time, the diagram already has even homology, so the result is manifestly in $\widehat{\mathcal{G}}^{\mathrm{ev}}(\mathcal{T})$. This also matches [AGLR, PP]. The authors in [PP] claimed that their calculation does not match with [AGLR], but their results are actually equal in $\widehat{\mathcal{G}}(\mathcal{T})$.

Finally, 3d-index of K_b is given by

$$I_M(K_b) = -q^{-1/2}\sum_{k\in\mathbb{Z}} 2q^k J_\Delta(2k,k,-1)J_\Delta(2k+1,k,0) + q^{2k}J_\Delta(2k,k,-1)^2. \tag{101}$$

Using methods described in [GHRS15, Section 7], we can find the first few terms in the series expansion.

$$-q^{1/2}I_M(K_b) = -3q - q^2 + 7q^3 + 15q^4 + 22q^5 + 11q^6 - 11q^7 - 60q^8 + O(q^9),$$
$$\iota(-q^{1/2}I_M(K_b)) = 1 - 3q - 6q^2 - q^3 + 9q^4 + 28q^5 + 39q^6 + 45q^7 + 20q^8 + O(q^9). \tag{102}$$

$\mathbb{L}_0$ $\mathbb{L}_1$
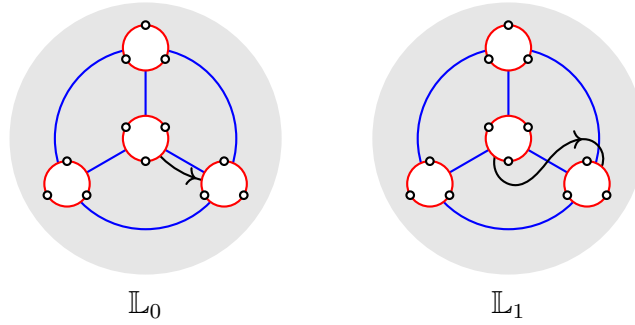
FIGURE 12. Lantern diagram for K_b.

The second line matches the calculations in [AGLR].

Acknowledgements. The authors wish to thank Tudor Dimofte, Thang Lê, and Mauricio Romo for enlightening conversations.

APPENDIX A. PROOF OF THEOREM 5.7

We only need to prove the theorem for a set of γ for which K_γ generates $\mathcal{S}(T^2)$. By [BP00], the skein algebra $\mathcal{S}(T^2)$ is generated by 3 elements K_m, K_l, K_{m+l} for some basis m, l of $H_1(T^2; \mathbb{Z})$. We start with the choice of m, l to make the diagrams as simple as possible, and then argue that quantum corrections vanish for these choices.

A.1. **Setting up the diagram.** The triangulation $\mathcal{T}$ induces a triangulation $\mathcal{T}_\partial$ of the boundary torus. The fundamental domain of $\mathcal{T}_\partial$ is (topologically) a parallelogram. Let m, l be the sides of the parallelogram with some orientation. They define a basis of $H_1(T^2; \mathbb{Z})$, and $m + l$ is a diagonal path of the fundamental domain. Let γ be any one of $m, l, m + l$. Then by pushing the path slightly to the right, we obtain a simple closed curve K_γ in general position with the 1-skeleton of $\mathcal{T}_\partial$. Moreover, there is at most one arc in each triangle of $\mathcal{T}_\partial$, and the arc is one of two types: a "small" counterclockwise arc or a "big" clockwise arc. See Figure 13.
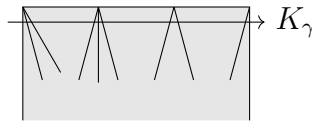
FIGURE 13. The curve K_γ.

The diagram $D_\gamma \subset \Sigma_{\mathcal{T}}$ for K_γ on the dual surface can be obtained by the process in [GY, Section 6.1], which we briefly recall here. $\Sigma_{\mathcal{T}}$ is obtained from $\mathcal{T}_\partial$ by truncating the vertices and rearranging the truncated triangles into lanterns. Note the curve K_γ avoids the vertices of $\mathcal{T}_\partial$. Then the process turns K_γ into D_γ. The punctures on the boundary triangles of lanterns correspond to the midpoints of edges of $\mathcal{T}_\partial$.

In this process, small arcs become standard arcs, and big arcs become arcs that are parallel to standard arcs but one click away at both endpoints. We call the second type *substandard*.

This is shown in Figure 14, where the blue dashed arc is the truncation at the vertex of $\mathcal{T}_\partial$, the blue solid arc is standard as usual, and the black arc is substandard.
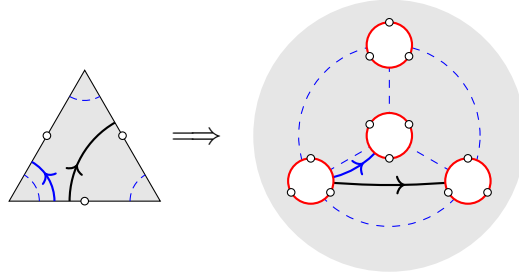

FIGURE 14. Standard and substandard arcs.

To calculate the quantum trace, we need to apply the splitting homomorphism to D_γ, and the choice of height orders for splitting is crucial. A convenient choice is to start at an intersection with an A-circle and assign monotonically decreasing height to D_γ. Right before coming back to the starting point, a sharp increase of height is needed to close up.

Since K_γ passes through each triangle of $\mathcal{T}_\partial$ at most once, the diagram D_γ has at most one arc in each region of the lanterns bounded by standard arcs. Then each boundary edge of the lanterns has at most 2 endpoints.

If there is a boundary edge with exactly one endpoint, then increasing height in the discussion above is actually irrelevant, since only the height order is preserved by isotopy. Then we can write

$$\Theta_A(D_\gamma) = \sum_{s_1,\ldots,s_k=\pm} D^1_{\gamma,s_1 s_2} \cup D^2_{\gamma,s_2 s_3} \cup \cdots \cup D^k_{\gamma,s_k s_1}, \tag{103}$$

where $D^i_{\gamma,\mu\nu}$ is the i-th arc of D_γ with states μ,ν at the starting and ending points, respectively. We call this type of γ type I. Here, $\cup$-product is used since the splitting (17) does not have the correction factor from (12).

If there is no such boundary edge, then we are forced to deal with the increasing segment. We use the trick of coaction, where we double the A-circle and put the segment in an annulus, which is later absorbed by the counit. By listing the finitely many combinations of standard and substandard arcs, we see that the two segments in the annulus always have opposite orientations. Therefore, the local picture looks like Figure 15. Then the result of splitting is

$$\Theta_A(D_\gamma) = \sum_{s_1,\ldots,s_k=\pm} \epsilon \left(\begin{smallmatrix} s_{t+1}\uparrow & & \\ & & s_t \\ s_k & & s_1 \\ & & \downarrow \end{smallmatrix} \right) D^1_{\gamma,s_1 s_2} \cup \cdots \cup D^{t-1}_{\gamma,s_{t-1}s_t} \cup D^{t+1}_{\gamma,s_{t+1}s_{t+2}} \cup \cdots \cup D^{k-1}_{\gamma,s_{k-1}s_k}. \tag{104}$$

As before, D^i_* denotes the i-th segment. The t-th and k-th segments are in the counit. We call this type of γ type II.

A.2. **Height exchanges and q-commuting relations.** The quantum trace $\widehat{\mathrm{tr}}_\mathcal{T}(K_\gamma)$ is obtained from the splitting by applying relations such as those in Lemma 2.1 to reduce everything to standard arcs. However, the fact that these relations only hold at the bottom (as a consequence of the left ideal) means we cannot reduce each arc independently in an obvious way. This issue is even more apparent in the calculation of $\widehat{\mathrm{tr}}_\mathcal{T}(K_\gamma \cdot \alpha)$.
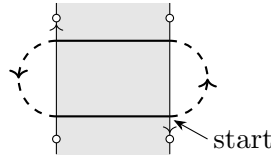
FIGURE 15. Local picture of 2 intersections with an edge.

A careful maneuver is required to bring the arc we want to reduce to the right end of the product. The moves below follow from [Lê18, Lemma 2.4], but we use form given in [LS, Equation (50)].

Lemma A.1. In $\mathcal{S}(\Sigma)$, we have the following height exchange moves.

$$\begin{array}{c}\mu\\\nu\end{array} = q^{\mu\nu/4}\begin{array}{c}\mu\\\nu\end{array} + \delta_{\mu<\nu}q^{-1/4}(q^{1/2} - q^{-1/2})\begin{array}{c}\nu\\\mu\end{array}. \tag{105}$$

$$\begin{array}{c}\mu\\\nu\end{array} = q^{-\mu\nu/4}\begin{array}{c}\mu\\\nu\end{array} + \delta_{\mu<\nu}q^{1/4}(q^{-1/2} - q^{1/2})\begin{array}{c}\nu\\\mu\end{array}. \tag{106}$$

The following corollary is checked by direct calculation. For convenience, we say a stated arc is *diagonal* if the states at both endpoints are the same.

Corollary A.2. The following q-commutation relations holds in the skein algebra $\mathcal{S}(\mathbb{L})$.

  (1) Suppose a, b are disjoint arcs with the same state at all 4 endpoints, then they q-commute.
  (2) Let a be an off-diagonal arc with endpoints on different boundary edges. Then a q-commutes with arcs isotopic to it but with possibly different states.
  (3) Suppose a and b are segments of D_γ in the same lantern, and a is standard. If a has $+$ and $-$ states at the starting and ending points respectively, then a and b q-commute.

Proof. (1) This directly follows from the lemma since $\mu = \nu$ implies that the second term vanishes for both moves.

  (2) This follows from the observations in [GY, Section 4.6].
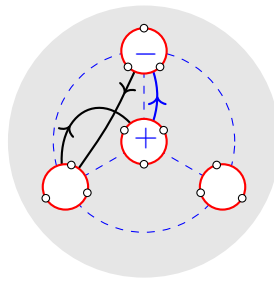
FIGURE 16. q-commuting positions for the standard arc.

  (3) If a and b do not have endpoints on the same boundary edge, then this follows from definition (12). If b is isotopic to a but with possibly different states, then this follows from (2). The only remaining cases are shown in Figure 16. Then the q-commuting property follows from direct calculations using the previous lemma.   □

Let c be a substandard arc on $\mathbb{L}$ with its "big clockwise" orientation. Define $c_{\mu\nu}$ as c with states μ and ν at the starting and ending points respectively. See Figure 17. By Lemma 2.1, c_{+-} (by itself) reduces to an off-diagonal standard arc in $\mathcal{S}_{\mathrm{cr}}(\mathbb{L})$ of the form in Corollary A.2(3).
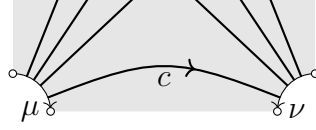

FIGURE 17. Locally picture of $c_{\mu\nu} \cup \alpha$.

For convenience, we call $\alpha \in \mathcal{S}_{\mathrm{cr}}(\mathbb{L})$ *standard off-diagonal* if it is a sum of products of standard arcs where each term has an off-diagonal arc.

Lemma A.3. Let α be a diagram on $\mathbb{L}$ disjoint from the substandard arc c up to isotopy.
  (1) If $(\mu, \nu) = (+, -)$, then c_{+-} and α q-commute in $\mathcal{S}(\Sigma)$.
  (2) If $\mu = \nu$, and α is a product of standard arcs, then in $\mathcal{S}_{\mathrm{cr}}(\mathbb{L})$, $(c_{\mu\mu} - s_{-\mu}) \cdot \alpha$ is standard off-diagonal. Here, $s_{-\mu}$ is the diagonal standard arc s parallel to c with state $-\mu$ at both endpoints.

Proof. The local picture of $c_{\mu\nu} \cup \alpha$ is given in Figure 17, and recall $c_{\mu\nu} \cdot \alpha$ differs from it by the factor in (12). For both parts, we need to apply Lemma A.1 repeatedly to bring certain endpoints to the lowest for corner reductions.

First look at (1). This is a more advanced version of Corollary A.2(3) and essentially the same proof as [CL22, Theorem 7.1]. On the $\mu = +$ side, we apply (105). Then the second term is 0 every time, so the entire height exchange is a single term with a power of q depending on which states are passed through. The $\nu = -$ side is similar. The result of the height exchanges is $q^k \alpha \cup c_{+-}$ for some k. Therefore, c_{+-} and α q-commute (for both $\cup$ and $\cdot$).

Next consider (2) with $\mu = \nu = +$. In anticipation of the application of Lemma 2.1, let d'_L and d_R be the gradings of α on the left and right edges in Figure 17, respectively. This also defines d_L, d''_L, d'_R, d''_R by the convention of Lemma 2.1.

The $\mu = +$ side is the same as (1) where the total power of q is $q^{d'_L/4}$. The $\nu = +$ side now has corrections from the second term of (106), but the leading term still safely move the $+$ state to the bottom with a factor of $q^{-d_R/4}$. In a correction term, $\nu = +$ passes through a $-$ state and the states get switched. This means the substandard arc becomes c_{+-}, so by part (1), it can be moved to the bottom, which then becomes standard off-diagonal after twisting, as mentioned before the lemma. Therefore,

$$c_{++} \cup \alpha = q^{\frac{1}{4}(d'_L - d_R)} \alpha \cup c_{++} + \alpha', \tag{107}$$

where α' is standard off-diagonal. Now we can twist c_{++} using Lemma 2.1 to get

$$\alpha \cup c_{++} = (\mathbf{i}q^{\frac{1}{8}(d_L - (d'_L + 1) + 3)})(-\mathbf{i}q^{\frac{1}{8}((d_R + 1) - d'_R - 3)})\alpha \cup s_- + (\text{off-diagonal term}). \tag{108}$$

The off-diagonal term comes from the $+$ state term in the second part of (16), which can be combined with α'.

Next, we try to flip the product order in $\alpha \cup s_-$. Standard arcs away from s $\cup$-commutes with s_-, and the rest of the standard arcs $\cup$-commutes with s_- up to standard off-diagonal terms. See e.g. [GY, Section 4.6]. Thus, $\alpha \cup s_- - s_- \cup \alpha$ is off-diagonal, and we can flip the $\cup$-product order in (108).

Finally, we can put in the factors from (12) for both $c_{++} \cup \alpha$ and $s_- \cup \alpha$. After everything is combined, we get

$$c_{++} \cdot \alpha = q^{\frac{1}{4}(d_L - d'_R)} s_- \cdot \alpha + \alpha'. \tag{109}$$

If α is already off-diagonal, then this shows $c_{++} \cdot \alpha$ is standard off-diagonal, and so is $(c_{\mu\mu} - s_{-\mu}) \cdot \alpha$. If α is indeed diagonal, then $d_L = d'_R$, so $(c_{\mu\mu} - s_{-\mu}) \cdot \alpha = \alpha'$ is standard off-diagonal. This proves part (2) for $\mu = \nu = +$. The case of $\mu = \nu = -$ is similar, so we omit the calculation here. $\qquad\square$

A.3. **Type I.** We start with the simpler case of type I γ.

Given $\alpha \in \mathcal{S}(M)$, the quantum trace $\widehat{\mathrm{tr}}_{\mathcal{T}}(\alpha)$ is represented by $\sum_i r_i \alpha_i$ where $r_i \in \mathbb{Z}[\mathbf{i}][q^{\pm 1/8}]$ and $\alpha_i \in \bigotimes_j \mathcal{S}_{\mathrm{cr}}(\mathbb{L}_j)$ is a product of standard arcs. Since the reduction from α to α_i happens "below" D_γ, we also have

$$\widehat{\mathrm{tr}}_{\mathcal{T}}(K_\gamma \cdot \alpha) = \sum_{s_1, \ldots, s_k = \pm} q^{w_s} D^1_{\gamma, s_1 s_2} \cdot D^2_{\gamma, s_2 s_3} \cdots D^k_{\gamma, s_k s_1} \cdot \sum_i r_i \alpha_i, \tag{110}$$

where w_s is the correction factor for turning $\cup$ into $\cdot$. Suppose not all states s_* are the same, then there exists some $(s_j, s_{j+1}) = (+, -)$, where $s_{k+1} = s_1$ for convenience. If $D^j_{\gamma, s_j s_{j+1}}$ is standard, then by Corollary A.2(3), it can be brought to the front of the product, so the term becomes 0 in $\widehat{\mathcal{G}}(\mathcal{T})$. If it is substandard instead, then we use Lemma A.3 to bring it to the bottom. As noted before Lemma A.3, by twisting it into a standard arc, Corollary A.2(3) applies again to show that the term is 0 in $\widehat{\mathcal{G}}(\mathcal{T})$.

This shows that there are only two potentially nonzero choices of states in (110). Take the all $+$ state term. We can twist the substandard segments of D_γ using Lemma A.3 from the lowest to the highest. If α_i is off-diagonal, then it is a 0 term in $\widehat{\mathrm{tr}}_{\mathcal{T}}(\alpha)$ by definition, and it is also a 0 term in (110) by Lemma A.3. If α_i is diagonal, then up to terms that will eventually become 0 in $\widehat{\mathcal{G}}(\mathcal{T})$, each substandard segment can be replaced by the corresponding standard arc with $-$ states by Lemma A.3. The same process is applied to the all $-$ state term, and we get

$$\widehat{\mathrm{tr}}_{\mathcal{T}}(K_\gamma \cdot \alpha) = \sum_{s = \pm} q^{w_s} \tilde{D}^1_{\gamma, s} \cdot \tilde{D}^2_{\gamma, s} \cdots \tilde{D}^k_{\gamma, s} \cdot \widehat{\mathrm{tr}}_{\mathcal{T}}(\alpha), \tag{111}$$

where $\tilde{D}^t_{\gamma, s}$ is the standard arc $D^t_{\gamma, ss}$ if the t-th segment of K_γ is counterclockwise, and it is the standard arc parallel to $D^t_{\gamma, *}$ with state $-s$ if the t-th segment of K_γ is clockwise.

The Weyl-ordering of the product of $\tilde{D}$ in (111) is the definition of $\hat{m}_\gamma^{\pm 1}$, so to prove the theorem, the last step is to show that the Weyl-ordering factor cancels q^{w_s}. This follows from the following claims.

(1) The original arcs $D^1_{\gamma, ss}, D^2_{\gamma, ss}, \ldots, D^k_{\gamma, ss}$ q-commute.
(2) The q-commuting relations of $\tilde{D}^*_{\gamma, s}$ are the same as $D^*_{\gamma, ss}$.
(3) $D^1_{\gamma, ss} \cup D^2_{\gamma, ss} \cup \cdots \cup D^k_{\gamma, ss}$ is the Weyl-ordering of $D^1_{\gamma, ss} \cdot D^2_{\gamma, ss} \cdots D^k_{\gamma, ss}$.

Now we establish the claims. (1) follows from Corollary A.2(1). (2) is checked by direct calculation since there are finitely many types of arcs. For (3), we need to compare the Weyl-ordering q^{w_s} with the factor from (12). Consider a pair $D^i_{\gamma,ss}$ and $D^j_{\gamma,ss}$ where $i < j$. The q-commutation between them has two sources. If they have endpoints on the same boundary triangle but not the same boundary edge, then the q-commutation comes from (12), so this part of Weyl-ordering factor matches. If they have endpoints on the same boundary edge, then the q-commutation comes from height exchanges. However, since these arcs arise from splitting, there is another pair of arcs on the other side with the opposite height exchange q-commutation. Thus, these two pairs have cancelling contributions to the Weyl-ordering, and they also have no contribution in (12). This proves (3).

A.4. **Type II.** Now we consider type II γ. The outline of the proof is the same, so we only explain the parts that are different.

The formula for the quantum trace is now

$$\widehat{\mathrm{tr}}_{\mathcal{T}}(K_\gamma \cdot \alpha) = \sum_{s_1,\ldots,s_k=\pm} q^{w_s} \epsilon \left(\begin{smallmatrix} s_{t+1} & & & s_t \\ s_k & & & s_1 \end{smallmatrix} \right) D^1_{\gamma,s_1 s_2} \cdots D^{t-1}_{\gamma,s_{t-1}s_t} \cdot$$
$$D^{t+1}_{\gamma,s_{t+1}s_{t+2}} \cdots D^{k-1}_{\gamma,s_{k-1}s_k} \cdot \sum_i r_i \alpha_i. \tag{112}$$

Again, if not all states are the same, then we can find $(s_j, s_{j+1}) = (+, -)$. If $j \neq t, k$, then the argument is the same as type I. If j is one of t, k, then the counit is zero using height exchanges. See also [LY, Lemma 4.7]. Thus, the only nonzero terms are again the ones with all $+$ or all $-$ states. In this case, the counit is $q^{-1/4}$ for both choices of states.

The twists of the substandard arcs are the same as before, which gives

$$\widehat{\mathrm{tr}}_{\mathcal{T}}(K_\gamma \cdot \alpha) = \sum_{s=\pm} q^{w_s-1/4} \tilde{D}^1_{\gamma,s} \cdots \tilde{D}^{t-1}_{\gamma,s} \cdot \tilde{D}^{t+1}_{\gamma,s} \cdots \tilde{D}^{k-1}_{\gamma,s} \cdot \widehat{\mathrm{tr}}_{\mathcal{T}}(\alpha). \tag{113}$$

Again, we need to argue that the factor $q^{w_s-1/4}$ is exactly the Weyl-ordering. Claims (1) and (2) are the same as before. Claim (3) is modified to say that the $\cup$-product times $q^{-1/4}$ is the Weyl-ordering of the $\cdot$-product. The proof is almost the same except when it comes to the boundary edge that contains the starting point. (12) still has no contribution on this edge, but the q-commutations do not cancel on this edge since s_1 is higher than s_t, while s_k is lower than s_{t+1}. The contributions on this pair of edges is exactly $q^{-1/4}$. This finishes the proof.

References

[AGLR]   Prarit Agarwal, Dongmin Gang, Sangmin Lee, and Mauricio Romo, *Quantum trace map for 3-manifolds and a 'length conjecture'*, Preprint 2022, arXiv:2203.15985.

[Bar99]   John Barrett, *Skein spaces and spin structures*, Math. Proc. Cambridge Philos. Soc. **126** (1999), no. 2, 267–275.

[BLF05]   Doug Bullock and Walter Lo Faro, *The Kauffman bracket skein module of a twist knot exterior*, Algebr. Geom. Topol. **5** (2005), 107–118.

[BP00]   Doug Bullock and Józef Przytycki, *Multiplicative structure of Kauffman bracket skein module quantizations*, Proc. Amer. Math. Soc. **128** (2000), no. 3, 923–931.

[CL22]   Francesco Costantino and Thang T.Q. Lê, *Stated skein algebras of surfaces*, J. Eur. Math. Soc. (JEMS) **24** (2022), no. 12, 4063–4142.

[CM19] Laurent Côté and Ciprian Manolescu, *A sheaf-theoretic* SL(2, ℂ) *Floer homology for knots*, Proc. Lond. Math. Soc. (3) **119** (2019), no. 5, 1336–1387.

[DGG] Zhihao Duan, Stavros Garoufalidis, and Jie Gu, *The descendants of the 3d-index*, Preprint 2024, arXiv:2301.00098.

[DGG13] Tudor Dimofte, Davide Gaiotto, and Sergei Gukov, *3-manifolds and 3d indices*, Adv. Theor. Math. Phys. **17** (2013), no. 5, 975–1076.

[DGG14] ———, *Gauge theories labelled by three-manifolds*, Comm. Math. Phys. **325** (2014), no. 2, 367–419.

[Dim16] Tudor Dimofte, *3d superconformal theories from three-manifolds*, New dualities of sypersymmetric gauge theories, Math. Phys. Stud., Springer, Cham, 2016, pp. 339–373.

[FG00] Charles Frohman and Răzvan Gelca, *Skein modules and the noncommutative torus*, Trans. Amer. Math. Soc. **352** (2000), no. 10, 4877–4888.

[GHHR16] Stavros Garoufalidis, Craig Hodgson, Neil Hoffman, and Hyam Rubinstein, *The 3D-index and normal surfaces*, Illinois J. Math. **60** (2016), no. 1, 289–352.

[GHRS15] Stavros Garoufalidis, Craig Hodgson, Hyam Rubinstein, and Henry Segerman, *1-efficient triangulations and the index of a cusped hyperbolic 3-manifold*, Geom. Topol. **19** (2015), no. 5, 2619–2689.

[GJS23] Sam Gunningham, David Jordan, and Pavel Safronov, *The finiteness conjecture for skein modules*, Invent. Math. **232** (2023), no. 1, 301–363.

[GKRY16] Dongmin Gang, Nakwoo Kim, Mauricio Romo, and Masahito Yamazaki, *Aspects of defects in 3d-3d correspondence*, J. High Energy Phys. (2016), no. 10, 062, front matter+99.

[GL] Stavros Garoufalidis and Thang T.Q. Lê, *From 3-dimensional skein theory to functions near* ℚ, arXiv:math.2307.09135, Preprint 2023, arXiv:2307.09135.

[GL16] Stavros Garoufalidis and Thang T. Q. Lê, *A survey of q-holonomic functions*, Enseign. Math. **62** (2016), no. 3-4, 501–525.

[GY] Stavros Garoufalidis and Tao Yu, *A quantum trace map for 3-manifolds*, Preprint 2024, arXiv:2403.12424.

[GZ] Stavros Garoufalidis and Don Zagier, *Knots, perturbative series and quantum modularity*, arXiv: 2111.06645, Preprint 2021, arXiv:2111.06645.

[GZ23] ———, *Knots and their related q-series*, SIGMA Symmetry Integrability Geom. Methods Appl. **19** (2023), Paper No. 082.

[Hab08] Kazuo Habiro, *A unified Witten-Reshetikhin-Turaev invariant for integral homology spheres*, Invent. Math. **171** (2008), no. 1, 1–81.

[HRS12] Craig Hodgson, Hyam Rubinstein, and Henry Segerman, *Triangulations of hyperbolic 3-manifolds admitting strict angle structures*, J. Topol. **5** (2012), no. 4, 887–908.

[Lê18] Thang T.Q. Lê, *Triangular decomposition of skein algebras*, Quantum Topol. **9** (2018), no. 3, 591–632.

[LS] Thang T.Q. Lê and Adam Sikora, *Stated sl(n)-skein modules and algebras*, Preprint 2022, arXiv:2201.00045.

[LY] Thang T.Q. Lê and Tao Yu, *Quantum traces for* SL_n*-skein algebras*, Preprint 2023, arXiv:2303.08082.

[Neu92] Walter Neumann, *Combinatorics of triangulations and the Chern-Simons invariant for hyperbolic 3-manifolds*, Topology '90 (Columbus, OH, 1990), Ohio State Univ. Math. Res. Inst. Publ., vol. 1, de Gruyter, Berlin, 1992, pp. 243–271.

[PP] Samuel Panitch and Sunghyuk Park, *3d quantum trace map*, Preprint 2024, arXiv:2403.12850.

[Prz91] Józef Przytycki, *Skein modules of 3-manifolds*, Bull. Polish Acad. Sci. Math. **39** (1991), no. 1-2, 91–100.

[Prz99] ———, *Fundamentals of Kauffman bracket skein modules*, Kobe J. Math. **16** (1999), no. 1, 45–66.

[RT91] Nicolai Reshetikhin and Vladimir Turaev, *Invariants of 3-manifolds via link polynomials and quantum groups*, Invent. Math. **103** (1991), no. 3, 547–597.

[Tur88]   Vladimir Turaev, *The Conway and Kauffman modules of a solid torus*, Zap. Nauchn. Sem.
          Leningrad. Otdel. Mat. Inst. Steklov. (LOMI) **167** (1988), no. Issled. Topol. 6, 79–89, 190.
[Tur94]   _____, *Quantum invariants of knots and 3-manifolds*, De Gruyter Studies in Mathematics,
          vol. 18, Walter de Gruyter & Co., Berlin, 1994.
[WZ92]   Herbert Wilf and Doron Zeilberger, *An algorithmic proof theory for hypergeometric (ordinary
          and "q") multisum/integral identities*, Invent. Math. **108** (1992), no. 3, 575–633.

Shenzhen International Center for Mathematics, Department of Mathematics, Southern University of Science and Technology, 1088 Xueyuan Avenue, Shenzhen, Guangdong, China
http://people.mpim-bonn.mpg.de/stavros
   Email address: stavros@mpim-bonn.mpg.de

Shenzhen International Center for Mathematics, Southern University of Science and Technology, 1088 Xueyuan Avenue, Shenzhen, Guangdong, China
   Email address: yut6@sustech.edu.cn